Experimental Searches for the Top Quark

Robert Hollebeek
University of Pennsylvania

1992 SLAC Summer School Lectures

Introduction

There are several interesting questions which one might ask about the top quark, and these are the ones which I would like to concentrate on for these lectures. For example, does the top quark really exist, and how strong is the current evidence for it? Is it possible that previous searches could have missed it because of anomalies in the decay branching ratios? How good are these searches, and what are the techniques which are required? Finally, once the top quark is discovered, how do you measure its properties, and how much can be learned from these studies? Before going further into these discussions however, I would like to pause for a moment and suggest that perhaps the most interesting question is why is the top quark so heavy? Quoting from a paper by G. Kane, "In a naive standard model approach, probably all masses ought to be within a factor of two or so of Mw," so from a theorist's point of view, the proper question may well be why are all quarks except the t relatively light! Either way, the situation is curious, that the top quark mass is at least 18 times heavier than any other quark mass, and we have little idea why this is so. I would suggest that if the top quark is the only very heavy quark, and that its mass is close to the weak scale, that this is an important clue about the mechanism for generating quark masses.

Evidence for the Top Quark

There are three major items which give us rather good confidence that the top quark does indeed exist: the branching ratio for b decays to lepton pairs, the forward backward asymmetry of b quark production in e^+e^-, and the Z decays to b pairs. They all come from measurements of the properties of b mesons.[1] If the b quark is a singlet, we expect the branching ratio for b decays to lepton pairs to be greater than 1.3 10^{-2}. The Standard Model value on the other hand, where the b quark is a member of a doublet (i.e., the t exists), is 10^{-4} times smaller. Present limits from the CLEO experiment give a 90% CL limit of less than 1.2 10^{-3}. [2]

The forward-backward asymmetry in b quark production from e^+e^- is proportional to

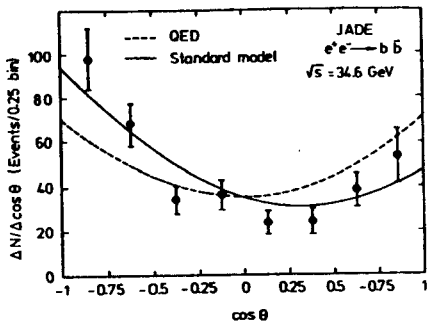

Figure 1: Direct measurements of the b quark asymmetry from jets produced at Petra.

$$T^b_{3L} - T^b_{3R}$$

from which one can conclude that the asymmetry would be zero for a b quark which is an isosinglet. Figure 1 shows the comparison of the data, with the expected asymmetry from the isodoublet structure as measured for b jets by the JADE collaboration, and the expected energy dependence of the effect as the energy approaches the Z resonance. Measurements made prior to the data taken by LEP detectors gave a value for the asymmetry of

$$T^b_{3L} = -0.54 \pm 0.13$$

where the value expected from the Standard Model is 1/2. The LEP data gives[3]

$$A^b{}_{FB} = 0.126 \pm 0.022$$

which is also consistent with expectations as show in Figure 2.

Further evidence for the existence of the t quark comes from the observation of Z decays to b quark pairs. The Z branching ratio for this process depends on the weak isospin quantum numbers of the b quark as

$$\Gamma(Z \to b\bar{b}) \sim 24\Gamma_0 \left[\left(T^b_{3L} + \frac{1}{3}\sin^2\theta_W \right)^2 + \left(\frac{1}{3}\sin^2\theta_W \right)^2 \right]$$

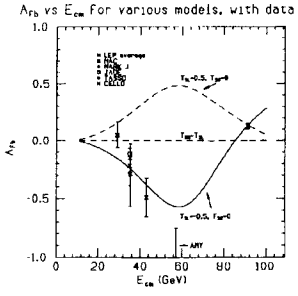

Figure 2: The forward-backward asymmetry as a function of center-of-mass energy.

with

$$\Gamma_0 = \frac{G_\mu M_Z^3}{24\pi\sqrt{2}} \sim 82.9 \text{ MeV}$$

when using a value for the weak mixing angle of

$$\sin^2\theta_W = .234 .$$

The predicted values of the branching ratio are then

$$\begin{array}{ll} T_{3L}^b = \frac{1}{2} & \Gamma = 367\text{MeV} = 0.126 \pm 0.022 . \\ T_{3L}^b = 0 & \Gamma = 24 \text{ MeV} \end{array}$$

The measured value

$$\Gamma_{exp} = 362 \pm 19 \text{ MeV}$$

clearly favors the weak isospin assignment which requires the b quark to have a partner.

There are also several theoretical arguments for the existence of the t within a Standard Model. For example, an anomaly free Standard Model requires that the sum of the family charges be zero. Given the b quark and the tau, there should be a charge 2/3 quark. Flavor changing neutral currents (FCNC) are suppressed by the GIM mechanism provided each family has the same singlet/doublet isospin structure. Without this suppression, FCNC should be observed in the B mesons well above observed limits. As a reminder, the GIM mechanism requires all L and R quark components of the same electric charge in different families to have the same weak isospin.[4]

Further evidence comes from $B\overline{B}$ oscillations. These oscillations from B to $\overline{B}$ proceed in second order weak via the exchange of virtual top quarks[5] with a mixing given by

$$x = \frac{\Delta M}{\Gamma} = \frac{\tau_B G_F^2 m_B}{6\pi^2} B_B f_B^2 \left|V_{td} V_{tb}^*\right|^2 m_t^2 F\left(\frac{m_t^2}{m_W^2}\right) \eta_{QCD} .$$

The Argus detector with three mixed events and one unmixed event gives a value of x of

$$x = (0.72 \pm 0.15) ,$$

and an r value of

$$r = 20.6 + -7.0\%$$

where x and r are related by

$$r = \frac{x^2}{2 + x^2} .$$

The ratio of mixing probability to total is χ which is related to r via

$$\chi = r/(1 + r) .$$

In the formula for x, the B lifetime, B mass, F, and the QCD correction are relatively well known. The value of V(tb) is probably close to unity. The B meson decay constant f_B and the bag parameter B_B are not so well known. The measurement of x can however give some information about a missing element of the KM matrix namely V(td). The observed large B mixing is actually an indication of a fairly large t mass since the mixing increases quadratically with t mass.[6] The cdf value for B mixing is[7]

$$\chi = 0.176 \pm 0.031 \pm 0.032$$

while the ALEPH group sees

$$\chi = 0.129 \pm 0.022 .$$

The mass of the top quark often affects the cross section for other processes through radiative corrections. This provides indirect means to measure the top quark mass or place limits on it. An excellent example of such a process is the ratio

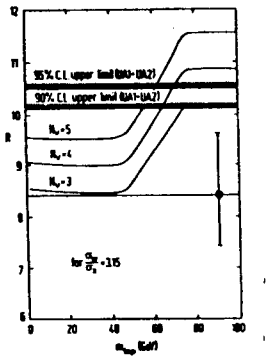

Figure 3: Measured and expected values of the ratio of leptonic Z's and W's as a function of the top mass.

of W and Z cross sections. The Z and W production cross sections each depend on m(top) but in different ways. By taking a ratio, some of the dependence on theory as well as the dependence on structure function uncertainties cancels. Using the dilepton detection mode for the Z and the single lepton plus missing Et for the W, the ratio is

$$R = \frac{\sigma_W}{\sigma_Z} \frac{\Gamma(W \to \ell\nu)}{\Gamma(Z \to \ell\ell)} \frac{\Gamma_Z}{\Gamma_W}.$$

By measuring this ratio (see Figure 3), and using the Standard Model to calculate the branching ratios of Z's to lepton pairs and W's to leptons plus neutrinos, one can solve for the ratio of the total width of the Z and W. This total width will in turn depend on whether the t quark is light enough to open the t pair channel for the Z or the tb channel for the W decay. Using the measured total width for the Z, the width calculated for the W is too low to be consistent with an open channel for W decays to the t and shown in Figure 4.

The value of the W mass also depends on the mass of the t quark through radiative corrections. In general, the W mass gets heavier as the top mass gets heavier as shown in Figure 5. Actually the problem is somewhat more complex because as is typical in such calculations, the W mass depends not only on the top mass, but also slightly on the assumed mass of the Higgs. As might be expected,

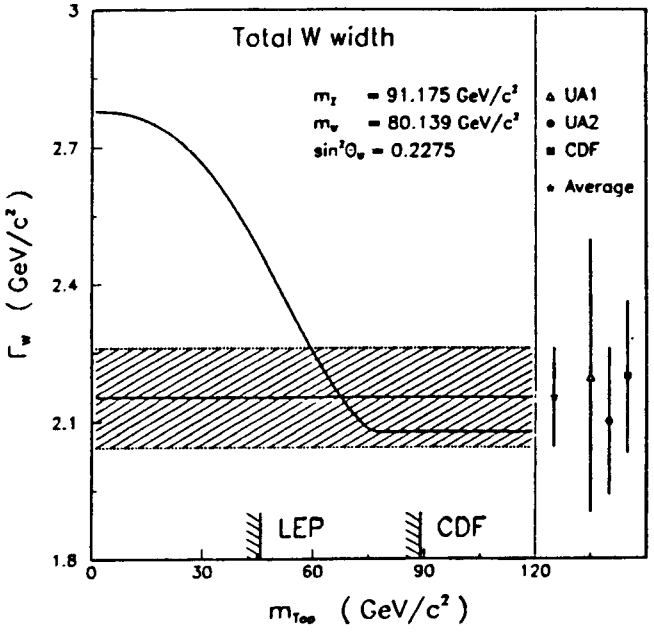

Figure 4: The total width of the W as a function of the top mass.

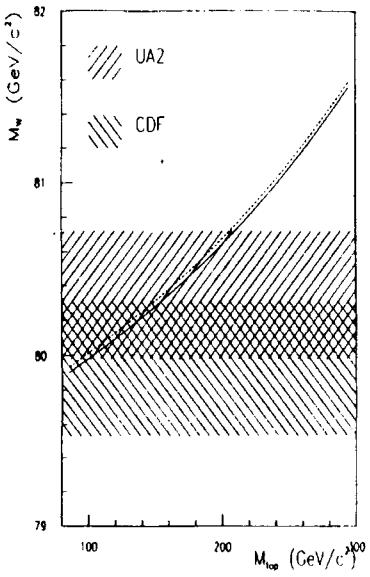

Figure 5: The measured W mass compared to the Standard Model predictions with dashed, solid and dotted curves corresponding to Higgs masses of 50, 100, and 1000 GeV.

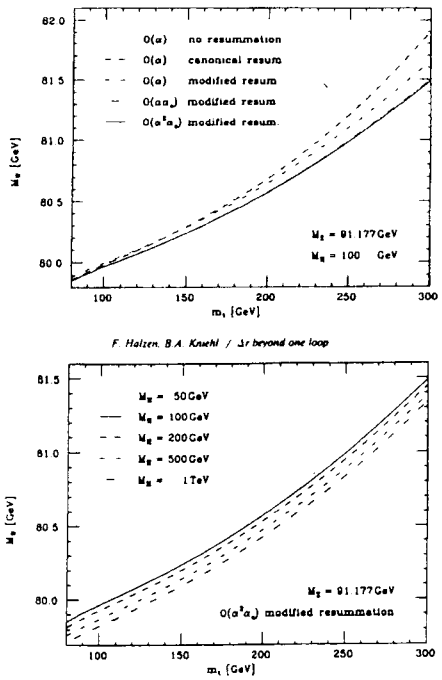

Figure 6: M_W vs. M_t for different calculations and different Higgs masses.

the heavier Higgs masses reduce the mass correction to the W (see Figure 6).

The Z partial width to fermions also depends on the value of the top and Higgs masses with corrections which are largest for the heavier masses like the b quarks.[8] Finally, the value of the weak angle is also changed by radiative corrections which depend on the mass of the top as shown in Figure 7.

Somewhat more unusual examples of processes with t quark dependence come from the $\pi\ \nu\ \nu$ decay of K mesons, and the $\gamma\ \gamma$ decay of the B_s. For the former process[9] the value of $\frac{\epsilon'}{\epsilon}$ is large and positive for mt=100 GeV, but is negative for mt=230 GeV. QCD corrections unfortunately will modify these predictions. For the two-gamma decay of the B_s, Figure 8 shows that the rate depends strongly on the top mass, changing by nearly a factor of two for top masses between Mw

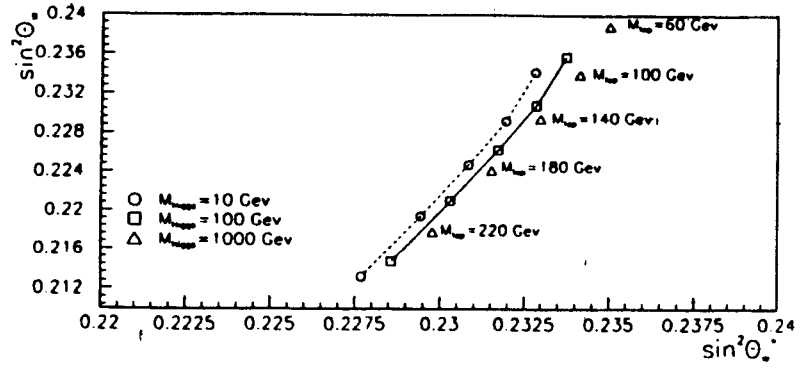

Figure 7: Predictions in the Standard Model for the Weinberg angles with various top and Higgs masses.

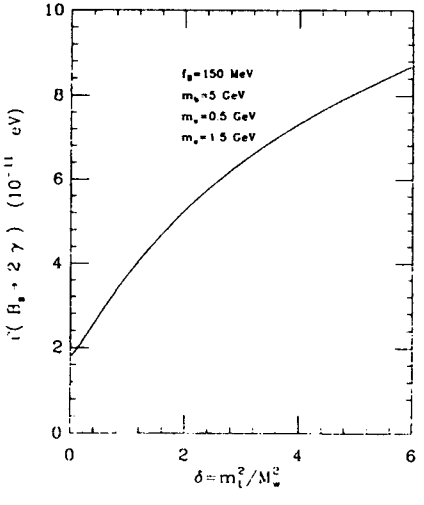

Figure 8: Dependence of the decay rate for $B_s \to \gamma\gamma$ as a function of the top mass.

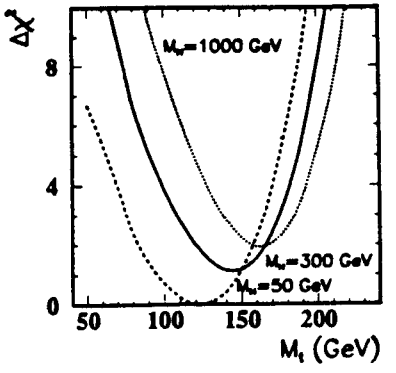

Figure 9: χ^2 curves as a function of top mass for combined fits to LEP data, M_W/M_Z UA2, M_W CDF, and CHARM data.

and 2 Mw.[10] Nevertheless, the branching ratio is quite small and difficult to measure.

Combined Fits

We can see then that there are a large number of parameters within the Standard Model which have some dependence on the top mass. Thus by combining all of the measurements made to date on standard model processes with a theoretical analysis of their dependencies on the top mass, it is possible to extract predictions for the allowable range and most likely value for this parameter. In an analysis by D. Schaile[11], the central value for the top mass is

$$m_t = 144^{+23+19}_{-26-21} \text{ GeV} .$$

Shown in Figure 9 are the chi-squared curves for these fits with different values of the top mass. Similar fits reported by Carter and Ellis at the Lepton Photon Conference gave[12]

$$m_t = 125 \textit{ to } 144 \pm 30 \text{ GeV}$$

$$m_t < 181 GeV [95\% \text{ CL}] .$$

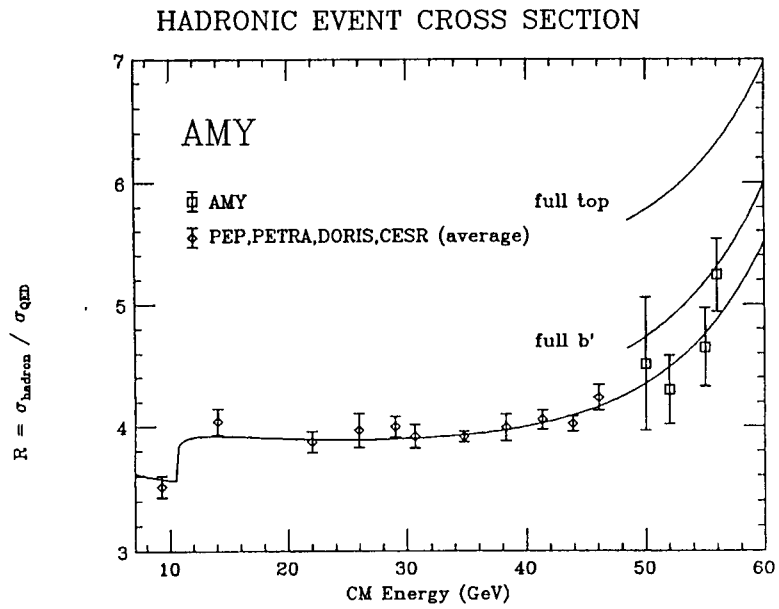

Figure 10: Low energy measurements of the e^+e^-hadronic cross section with predictions for the top contribution.

Other fits[13] also give values in the region of 130-140 GeV for the top mass with upper limits of 180-200 GeV.

The low mass region (below $\frac{M_Z}{2}$) can be probed for the existence of the top quark by looking at the production of quark pairs from e^+e^-annihilation (see Figure 10 and Figure 11). The presence of an additional quark would increase the value of R, the ratio of the total hadronic cross section to the point cross section. Objects like the t quark, which couple to e^+e^-electromagnetically, add an additional amount to this ratio proportional to their charge squared. As you can see, there is no evidence for a light additional quark.

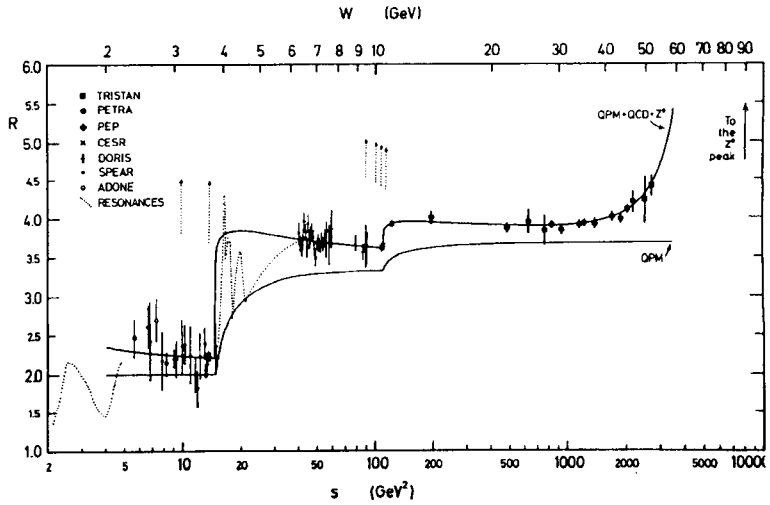

Figure 11: The ratio R of the hadron cross section in e^+e^- to the point cross section.

The process

$$Z \rightarrow t\bar{t}$$

is an excellent way to look for light t quarks, and the large number of available Z's allows the LEP experiments to exclude a top quark of mass less than 46 GeV at 95% confidence level with very little dependence on the way in which the t decays.

The highest mass limits, however, come from the CDF detector[14] which excludes a top quark with mass less than 91 GeV based on a Standard Model leptonic decay branching ratio of approximately 1/9. This is a mild assumption for t quarks heavier than the W since then most modifications of the t decay branching ratios do not substantially modify this leptonic mode.[15] Lower mass limits for the t decay from UA1 and UA2 relied on the production of t quarks in the decay of the W, which is the dominant t production mechanism at the lower energies which were available at the SpS.

t Quark Detection

The t quark has two principal decay modes: the leptonic decay, and the hadronic decay. The hadronic decays have a larger branching ratio, but are harder to detect than the leptonic mode, so that most experimental searches for the top quark depend on the leptonic decay of at least one t quark. Of the leptonic modes, the electron and muon decays are the most useful again because they are easily separated from jet backgrounds. One and three prong jets with low invariant mass are a reasonable signature for a tau lepton, but the background from QCD jets is high. In contrast, electron events can be found easily by using a good electromagnetic calorimeter. The chief backgrounds come from semi-leptonic decays of B mesons, the overlap of an energetic π^0 with an energetic charged track, and conversion electrons.

Since the top quark is now believed to be heavier than the W, the principal production mechanism will involve the production of a pair of top quarks. The top and the anti-top can each have either a hadronic or leptonic decay, and there are three leptons for the leptonic decay, so there are lots of potential final states and signatures for the top. Since the principal decay of the top is $t \rightarrow bW$, the final state probabilities can be understood by looking at the decays of the W. The W decays to three lepton types, and two quark families of three colors, with roughly equal probability for a total of nine possible final states. Ignoring mass effects which make small corrections to the rates for c quarks and tau leptons, the branching ratio for each mode is thus 1/9. From this, it is easy to estimate the relative frequency of various types of top decays. Dilepton events with the leptons coming directly from the decay of the W for example would have a probability of 1/9 * 1/9. Thus ee, $\mu\mu$, $\tau\tau$, all occur with the same rate namely 1/81. Dilepton events of the $e\mu$ type occur with twice this rate since there are two choices for which W has the e or μ decay i.e., 2/81. An event with a decay to an electron and an up quark, would occur with the same 1/9 * two choices * 1/9 but for each of three colors, so the rate becomes 6/81. Finally, for an electron plus jet decay, the jet can come from either an up quark or a c quark decay of the W which makes the rate 12/81 or 4/27=0.148. Corrections need to be made to these rates for leptons which do not come from the primary W (primarily from b decays). In the case of the 1989 CDF top search, as many as 30% of the electrons came from these secondary sources. This introduces some uncertainty in the detection efficiency due to uncertainties in the b quark branching ratios, but the effect is modest, and can be reduced by increasing the threshold on the transverse energy of the lepton.

The phenomenology of top decays which are much heavier than the W is quite different from that of light t quarks. In the Standard Model, the decay width of a light t is

$$m_t << m_W, \Gamma_t \sim \frac{3}{64}\frac{G_\mu^2 m_t^5}{\pi^3}$$

while for heavy t quarks it is

$$m_t >> m_W, \Gamma_t \sim 0.17\left(\frac{m_t}{m_W}\right)^3\left(1-\frac{m_W^2}{m_t^2}\right)^2\left(1+2\frac{m_W^2}{m_t^2}\right) .$$

As the top becomes heavier than the W, the decay to real W's accompanied by a b quark becomes the dominant decay mechanism. Figure 12 shows this rapid change in the b quark fraction as a function of the top mass.[16] Thus the presence

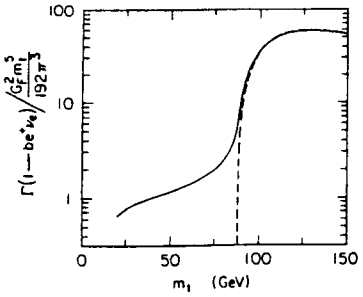

Figure 12: Leptonic width of the t as a function of the top mass.

of b quarks detected by vertex detectors can become a major tool in investigating the properties of the top.

Finally, where would one expect to find the top quark given the present state of theory? The cynical answer is that it is always predicted to be just a little heavier than current experimental limits so it remains tantalizingly out of reach! While preparing these lectures, I kept a plot of some of the theoretical predictions which I found for the top quark mass as shown in Figure 13. Some of the predictions are phenomenological fits to present data, and some are based on specific theories. The highest two predictions are based on supersymmetry which without modifications tends to predict a rather heavy top quark. Given that the present experimental limits are about 100 GeV, and that the next run of the Tevatron will cover up to about 150 GeV, the theoretical predictions seem well placed!

There are a number of other interesting constraints on the possible mass of the top quark. For example, the value of ϵ and ϵ' together with the branching ratio for $K \to \mu\mu$ predicts[17] that the mass of the top should be less than 350 GeV. The width of the Z would be sensitive to the existence of a new decay channel involving the top quark, and the value of the width together with the expected changes in the thrust and acoplanarity distributions (see Figure 14) allows the LEP collaborations to place a very model independent lower bound on the top mass of 46 GeV. As discussed previously, the W can be used in a similar fashion

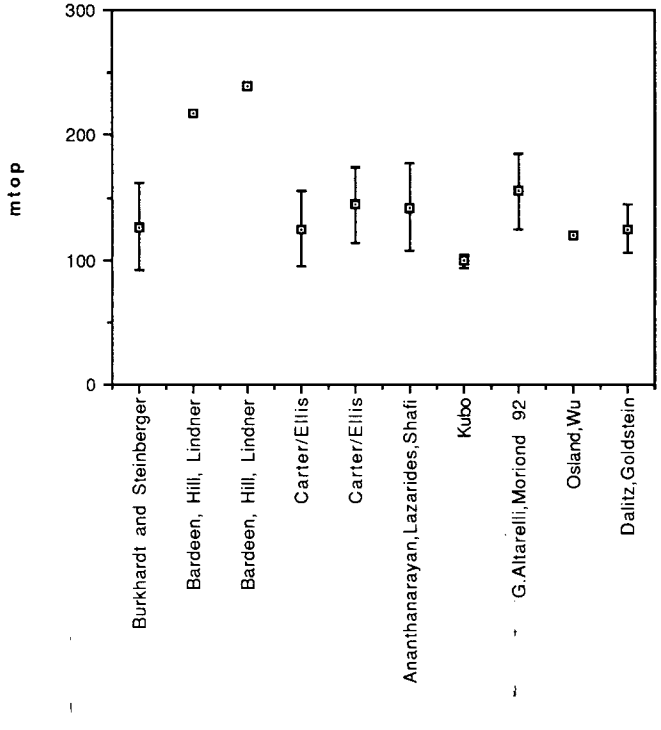

Figure 13: Collected predictions for the top mass.

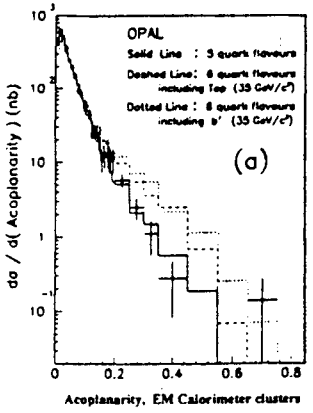

Figure 14: Event acoplanarity distribution (LEP-OPAL).

because the top quark contributes differently to the lepton partial widths of the Z and W. By using the ratio of W's and Z's detected in the leptonic channels, the total width of the W can be calculated from the ratio of the total W and Z production cross sections. The measured values give[18]

$$\Gamma_W^{exp} = 2.184 \pm 0.124 \text{ GeV} .$$

This should be compared to the Standard Model value without a contribution from the top of

$$\Gamma_W^{SMnotop} = 2.059 \pm 0.074 \text{ GeV} .$$

If the difference is attributed to a contribution from a top quark, then it yields the constraint

$$M_t > 52 \text{ GeV} .$$

Some constraints on the top mass do not rely on experimental measurements but are based on purely theoretical arguments. The unitarity of $t\bar{t}$ scattering requires[19] a top mass which is less than 500 GeV because the s wave amplitude is constrained by

$$\frac{3G_F m_t^2}{4\sqrt{2}\pi^2} < \frac{1}{2} .$$

The requirement of vacuum stability within the Standard Model[20] can constrain the top mass because if the top mass is too large, the vacuum decays in a time less than the lifetime of the universe unless

$$m_t < 95 \text{ GeV} + 0.6 m_H$$

where m_H is the Higgs mass.

By combining these experimental measurements and the theoretical expectations within the Standard Model parameterized as functions of the top and Higgs masses, Langacker and others have been able to place constraints on these masses.[21] The basic inputs are the following:

muon lifetime,

Z mass,

W mass (with errors expected to improve from about 400 MeV at present to between 50 and 100 MeV using new data from the Tevatron),

Z total and partial widths,

Z production cross section,

Z asymmetries,

νN and νe scattering data,

polarized lepton scattering,

atomic parity violation, and

PEP, PETRA, and TRISTAN cross sections and asymmetries.

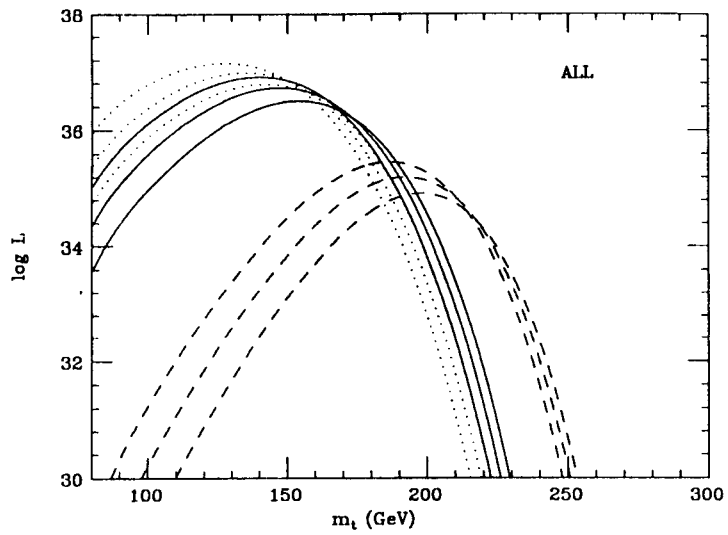

Figure 15: Log of the likelihood distribution as a function of top mass for higgs mass of 42 (dotted), 100 (solid) and 1000 (dashed) and $M_z = 91.177 \pm 0.031$. The three curves correspond to $M_z \pm 1\ \sigma$.

The result for the top mass depends on the values chosen for the Higgs mass as well as the strong coupling constant. For

$$M_z = 91.177, M_h = 100, \alpha_s = 0.120$$

the most likely value for the top mass is 147 GeV with a 95% CL upper limit of 186 GeV. Further improvements may require higher order loop corrections in the theoretical calculations, and will certainly benefit from the improvements expected in the W mass. Figure 15 shows the resulting log-likelihood function for the top mass.

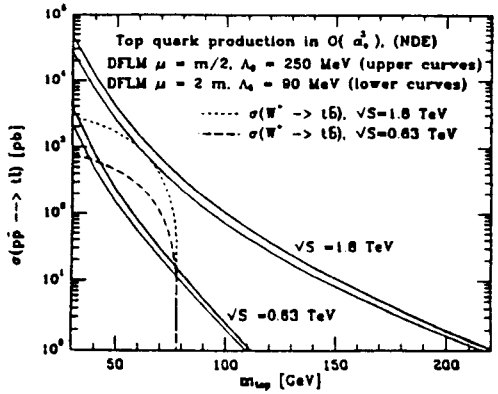

Figure 16: Production mechanisms for top at CERN and FNAL.

CDF Searches

The principal production mechanisms for the top at hadron machines are the decay from the W for light top, and pair production. UA1 and UA2 searches at CERN relied primarily on the W production cross section with light top decay products from the W as the primary top production mechanism. This was primarily because for the lower energies available at CERN at the time, the W production cross section with subsequent top decay was larger than the top pair cross section. As shown in Figure 16, the top pair cross section is much larger at the higher energies available at the Tevatron, and for top which is heavier than about 76 GeV, the

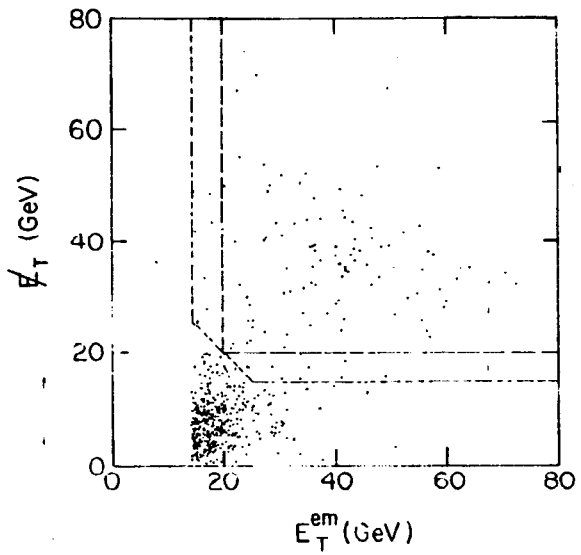

Figure 17: CDF electron candidates, $\not\!\!E_T$ vs. electron E_t.

W branching ratio to top becomes too small to be useful. The CDF collaboration used three primary modes for the top search:

1. electron + jets final states,
2. electron muon events, and
3. dileptons (ee, $\mu\mu$).

Electron + Jets

The observed distribution of events containing a high transverse momentum electron and missing transverse energy (shown in Figure 17) is strongly suggestive of two sources for these events. W production produces events with both large electron transverse energy (E_t) and large missing energy ($\not\!\!E_T$). B meson production explains the remainder of the events with low E_t and low $\not\!\!E_T$. The electromagnetic and hadronic calorimeters are used to select electron candidates. As shown in Figure 18, the hadronic fraction of the total energy should be small for an electron. Conversion pair backgrounds and electrons from the Z were eliminated by using invariant mass cuts and by using the Vertex Time Projection Chamber (VTPC) to identify conversion electrons which converted in the thick outer walls of the VTPC. Electrons from B meson sources are reduced by requiring the electron to be isolated. Because of the smaller mass of the b quark when compared to the t, the non-leptonic decay products of the b do not have as large a transverse momentum relative to the lepton. This causes additional tracks and or calorimetric energy to accompany the lepton at relatively small angles. Typical isolation cuts involve a cut either on the total energy in a cone around the direction of the electron, or the more efficient procedure of cutting on the energy in the calorimetric towers which border the tower hit by the electron candidate. A candidate electron must also have a detected track in the Central Drift Chambers (CTC) with a momentum which matches the calorimeter energy except for the radiative tail as shown in Figure 19. Strip chambers inside the electromagnetic calorimeter at a depth of about six radiation lengths measure the transverse shower profile which must have a good chi-square for its shape when compared to a sample of real electrons. The shower position must also match the extrapolated position of the charged track.

Because the proton anti-proton collision allows large amounts of momentum to be missing along either beam direction, the total longitudinal momentum of any event is unknown. Thus only the transverse components of the neutrino momentum vector from the W decay can be inferred, and it is not possible to calculate the invariant mass of the W from the electron and the $\not\!\!E_T$ vector. Instead, the invariant mass of the $e\nu$ system is calculated ignoring both the longitudinal momentum of the electron (known) and the neutrino (unknown). The invariant mass calculated in this way is called the transverse mass and is given by

$$M_T^{e\nu} = \sqrt{2E_T^e E_T^\nu (1 - cos\phi_{e\nu})} \; .$$

The distribution of this variable will roughly follow the mass of the parent object. For W's with no transverse momentum which decay at 90 degrees for example, the transverse mass will be the W mass within experimental errors. For other

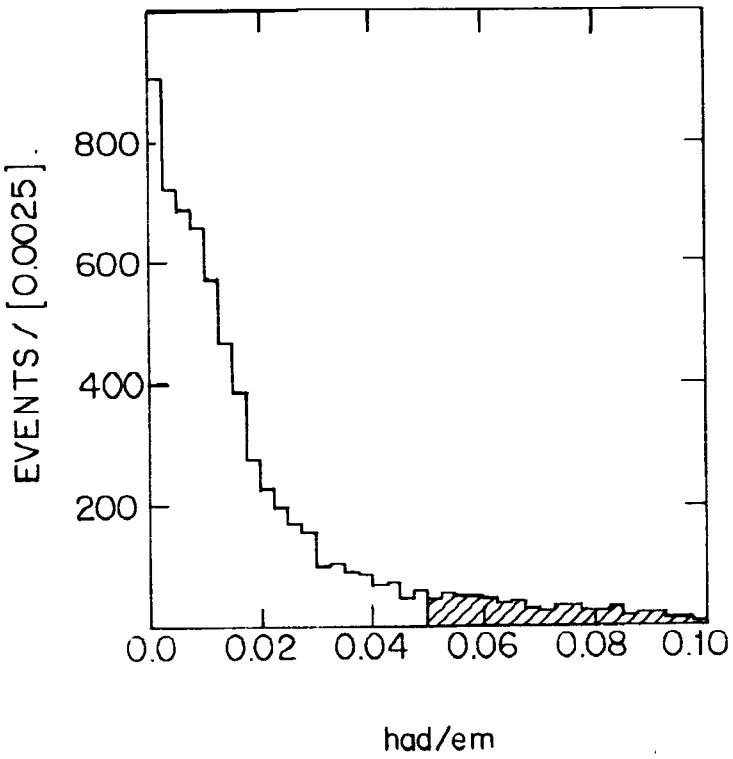

Figure 18: had/em distribution, CDF electron candidates. The hatched region is cut.

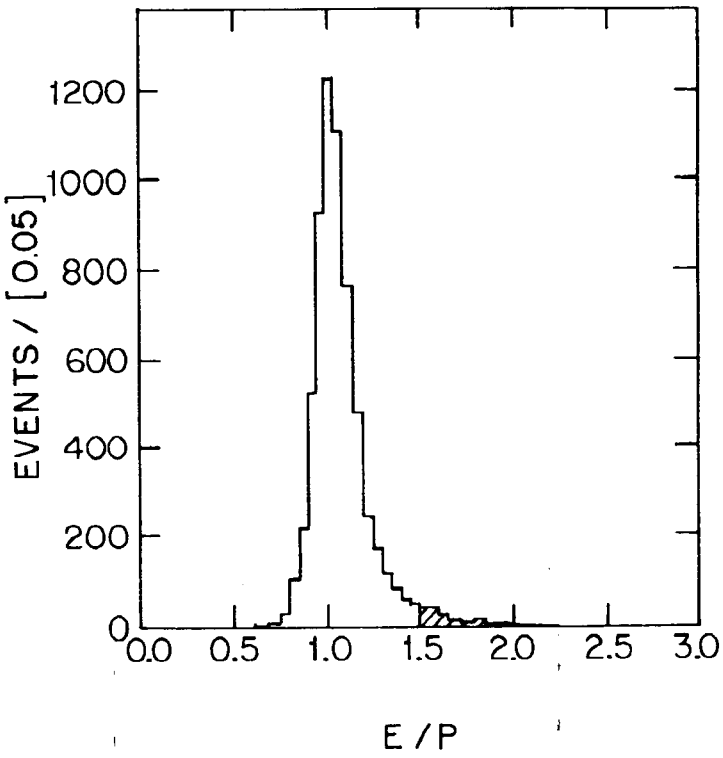

Figure 19: E/p distribution for CDF electron candidates.

angles, it should be less than the W mass. High p_t W's will contribute to a tail on the high mass side of the distribution as would a heavy object. A light object might produce an enhancement at lower values. Thus one would expect that events originating from a top quark which has a mass different from that of the W, would modify the shape of the overall distribution.

To improve the signal to background ratio, W events are suppressed and top events enhanced by requiring two jets in addition to the electron and $\not\!\!E_T$. Figure 20(a) shows the measured distribution together with the shapes expected for W's with two jets and for a 70 GeV top. Figure 20(b) shows the same distribution for the electron plus one jet sample which is dominated by W's and can therefore be used to provide some confidence that the corrections for W and top initial transverse momentum as well as experimental resolution are done properly.[22] The electron plus jets top search provides the single most stringent limit on top production and as shown in Figure 21 the region between 40 GeV and 77 GeV is excluded at 95% CL.

CDF $e\mu$ Search

The advantage of looking for the top in the electron muon channel is that both the electron and the muon have reasonably good signatures and can be detected with high efficiency. Compared to other dilepton channels, the electron muon channel also does not have opposite charge backgrounds from Drell-Yan production or from Z production. The systematic uncertainties associated with requiring a muon rather than a jet along with an electron are also smaller. At modest energies, the muon momentum resolution for the muon is not as good as the electron but is better than the systematic errors associated with measuring the energy of a jet. The CDF search required a high p_t (> 5 GeV) muon and an electron with p_t greater than 15 GeV with opposite charge.[23] The spectrum of minimum electron or muon momentum, pt_{min}, expected from $B\overline{B}$ sources and from low and high mass top is shown in Figure 22. Backgrounds from B mesons will dominate at low p_t. The top search uses a cut on p_t of 15 GeV for both the electron and the muon. One candidate event survives the cuts with electron E_t of 31.7 GeV and muon E_t of 42.5 GeV. As seen in Figure 23 which plots the electron E_t versus the muon E_t,

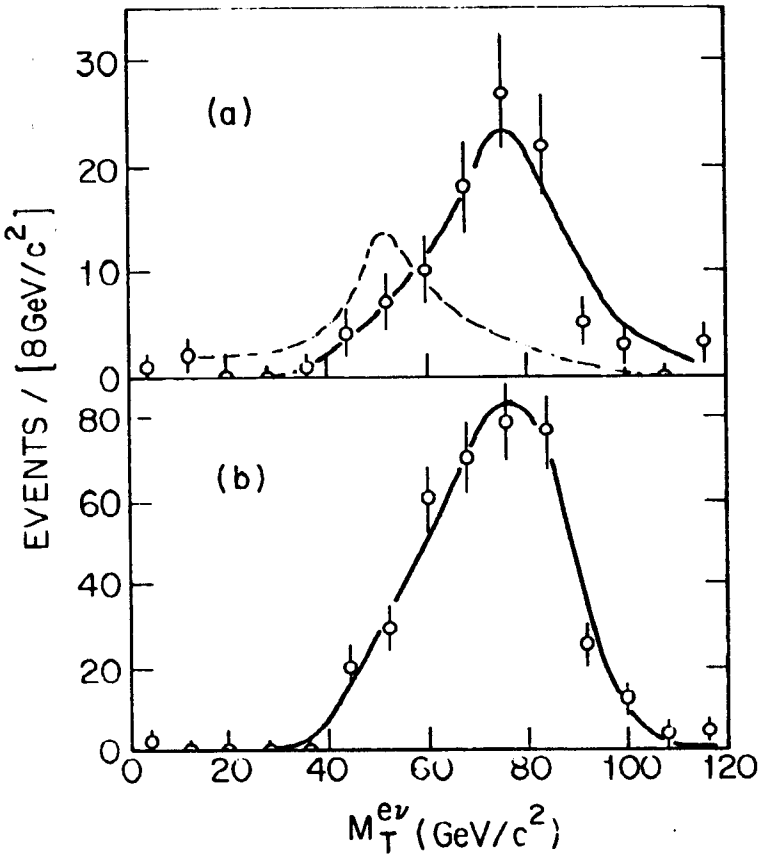

Figure 20: Transverse mass distributions for CDF electron plus two jet sample and effect of a 70 GeV top (a), and the distribution for the W plus one jet sample (b).

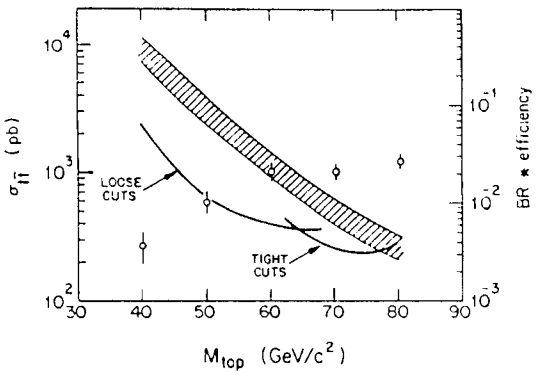

Figure 21: CDF electron plus jets limit on top production.

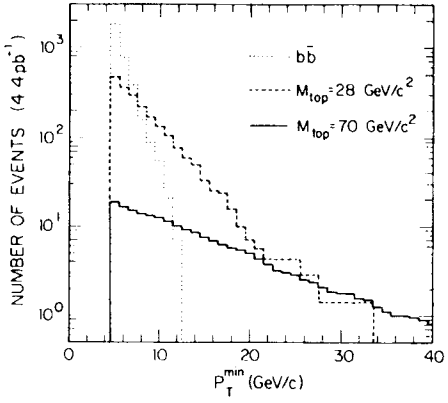

Figure 22: The Monte Carlo expected p_t distributions for opposite charged electron muon events from top and $b\bar{b}$ production. The integrated luminosity corresponds to the CDF sample.

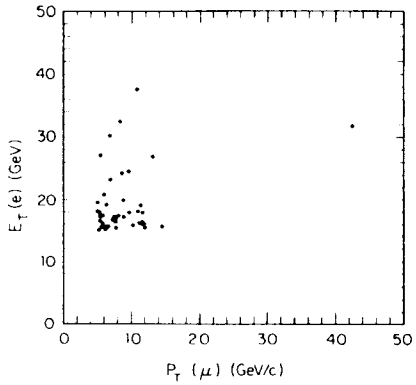

Figure 23: Electron transverse energy versus muon transverse momentum for the CDF data.

the event is unusual. The event also has a second muon candidate in the forward muon detector as well as a jet with 14 GeV E_t. This one observed event, combined with the systematic uncertainties in the efficiency, uncertainties in the value of the production cross section, and fragmentation effects, yields a 95% CL limit $M_t > 72$ GeV.

Dilepton Searches

Electron and muon pair events contain substantial backgrounds from Drell-Yan pairs and from Z decays. The Z decays can be removed by making a cut on the pair invariant mass between 75 and 105 GeV. To further reduce backgrounds, events are required to have missing E_t greater than 20 GeV as would often be the case in top pair events with dileptons where there are also at least two neutrinos. Low p_t Drell-Yan pairs are reduced by requiring that the lepton pair should not be back-to-back. This also reduces $B\overline{B}$ and QCD backgrounds. The cut requires $20 < \Delta\phi < 160$. The lower limit for the top mass from the combined electron and muon channels is 84 GeV. Further improvement in the limit (to 89 GeV) comes from combining this result with a search for electron or muon events with both jets and an additional soft muon candidate as shown in Figure 24.

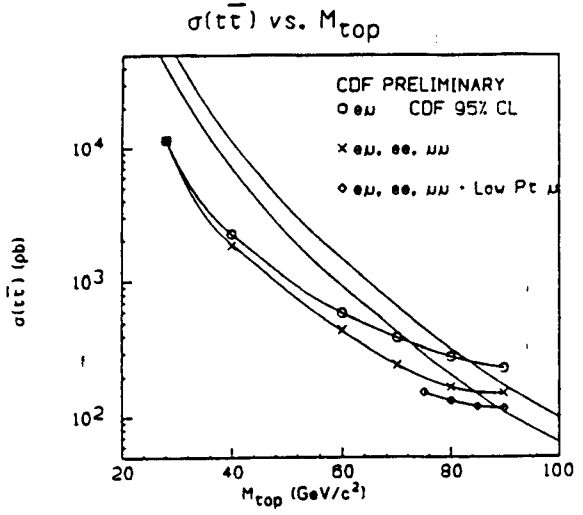

Figure 24: Top quark limits from dilepton samples, CDF.

As the search for the top quark proceeds to heavier and heavier masses, the production cross section of the missing top becomes smaller and smaller. The cross section for 90 GeV top production is ten times larger than that for a mass of 140 GeV which is in turn ten times larger than the 200 GeV cross section. As a result, the search techniques used must rely on additional details of the top signature to help separate it from the backgrounds. Fortunately heavier top quarks produce higher p_t jets and leptons which helps. One of the strategies which is being investigated to improve the sensitivity of these searches is to add a muon to the electron plus jet search, or if you will, add jets to the electron muon search. Another strategy would be to look for an electron or muon plus three jets. This signature, for example, would help reduce W plus jet backgrounds in the electron plus jets sample. Systematic uncertainties due to jet energy scale corrections remain a challenge as do the uncertainties in QCD corrections for W plus multijet backgrounds. Vertex tagging is another excellent technique for improving the top signature. Top pair events should also contain two b quarks, whose decays might be detected with such a detector. In principle, one would

Run	Luminosity	top mass
1992	25 pb^{-1}	120
1993	75	160
1995	325	200

Table 1: Tevatron Goals

like to see a sample of top-like events with either extended vertices in some jets, or reconstructed B mesons. Soft lepton tags have also been investigated since there are two tops, each with potential leptonic decays as well as two b quarks with direct or sequential leptonic decays. One would thus expect that top quark events would contain larger numbers of soft leptons and that multi-lepton events would be a good signature. Because of the softening momentum spectrum of such sequential decay products however, if one requires substantial momentum in for example three leptons, the overall efficiency becomes too small. The efficiency can be improved by looking for softer leptons but only if the backgrounds to the identification of such leptons can be well understood.

The increased integrated luminosity expected from the upcoming runs of the Tevatron should allow for the exploration of the entire mass region which seems consistent with our current theories (see Table 1). Improved detectors in the case of CDF and the addition of the D0 detector should greatly improve the prospects for finally measuring the properties of the top quark. It is interesting to note that as the instantaneous luminosity increases, detectors will need to learn to handle the situation of having more than one interaction in a single bunch crossing. Since the total cross section for $p\bar{p}$ is 46 mb, the number of interactions per bunch crossing is given by

$$\mathrm{L}(10^{31})\ \ 46\ 10^{-26}\ \ 3.5\ 10^{-6}\ .$$

Measuring the Mass of the t

Let's suppose that our goal is to make a 5% or better measurement of the mass of the top quark. Given the present limits, this would imply an absolute error of between 5 and 10 GeV. QCD corrections for the production cross section would be required because they typically contribute 10% effects.[24] The easiest way

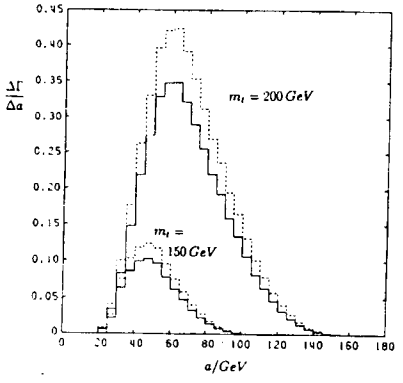

Figure 25: Histogram for the distribution of $\Delta\Gamma/\Delta a$ for 150 GeV and 200 GeV top masses; lowest order (dashed), including first order QCD (solid).

to measure the top mass is to relate it to the inclusive lepton spectrum. The disadvantages of using this measurement is that the spectrum depends on both the unknown p_t spectrum of the produced top quarks and on the spectrum of secondary leptons from sequential decays (i.e., leptons from b or c quarks). The latter effect requires a knowledge of both the branching ratios and the spectra for these secondary decays.

In final states which involve dileptons, it is also possible to relate the top mass to the dilepton invariant mass distribution. Some uncertainty in the top mass (2-3%) remains due to uncertainties in the contributions from secondary leptons. Again, information is needed on the p_t of the top, the fragmentation spectra for the quarks, and possible polarization effects. The measured inclusive lepton spectrum from B decays can be used to help constrain these effects. Corrections due to the width of the top quark itself are small. Figure 25 uses a million top events to illustrate this technique. The sample requires 30 GeV in one of the leptons, and at least 10 GeV in the other as well as a cut on the cosine of the angle between the pair of 0.8. The plot shows the expected distribution for 150 and 200 GeV top masses. The remaining error due to B fragmentation effects is estimated to be 1%. Uncertainties due to QCD are still 5%.

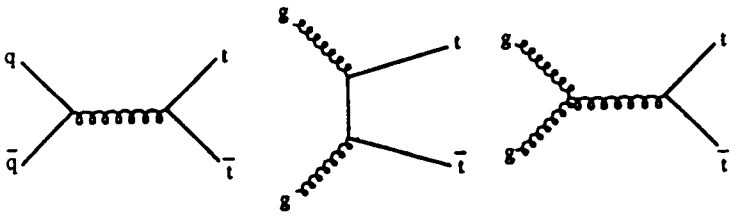

Figure 26: Lowest order diagrams for top production.

Production of the Top Quark

The lowest order diagrams for top production from $p\bar{p}$ are shown in Figure 26. The relative importance of the quark and gluon diagrams depends on the mass of the top. Heavier masses suppress the glue-glue contribution. Since this contribution has larger systematic errors, these errors reduce slightly as the top mass increases. This situation is most easily understood by remembering that the parton cm energy squared is x_1x_2s, where s is the $p\bar{p}$ center-of-mass energy and the x's are the parton energy fractions. Higher mass top requires larger x_1x_2. Since the glue to quark ratio decreases with increasing x, the glue-glue luminosity decreases for large top mass. Systematic uncertainties are smaller for large x as well as for quark distributions.

Figure 27 shows the production cross section for two different choices of the structure functions (one curve is divided by ten)[25] and shows that the cross section varies weakly with the choice of parton distribution parameterization and choice of scale. The vertical bars represent the change from using a scale equal to the mass of the top and one equal to twice the mass of the top. The dependence of the top cross section on scale[26] shown directly in Figure 28 illustrates that the scale dependence is often smaller in calculations with higher order corrections. Uncertainties in the cross section for higher energy machines like the LHC and SSC are larger because as shown in Figure 29 the higher energies increase the fraction of the cross section which comes from glue-glue. The glue-glue process dominates at the SSC because the top mass is smaller relative to the cm energy of

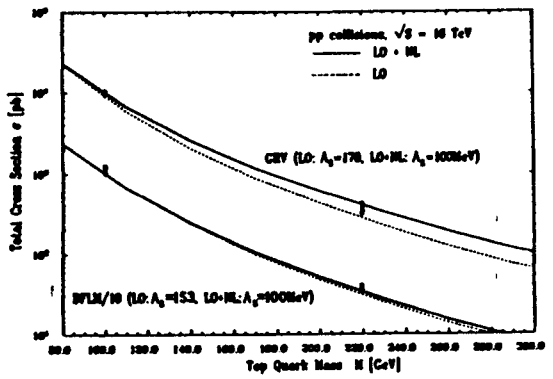

Figure 27: Predictions for the top quark cross section.

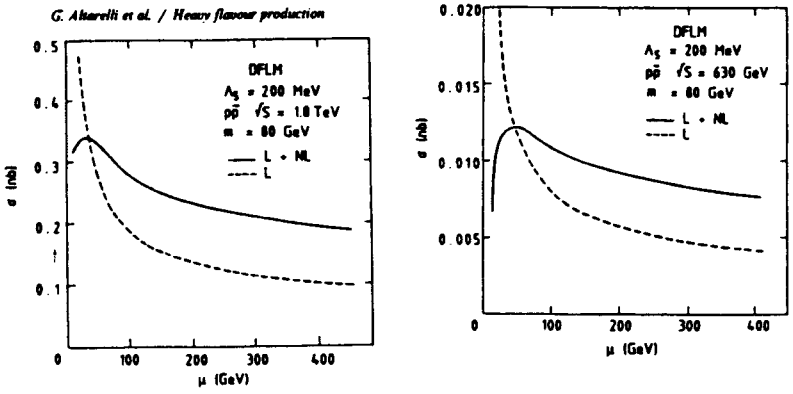

Figure 28: μ dependence of the top cross section.

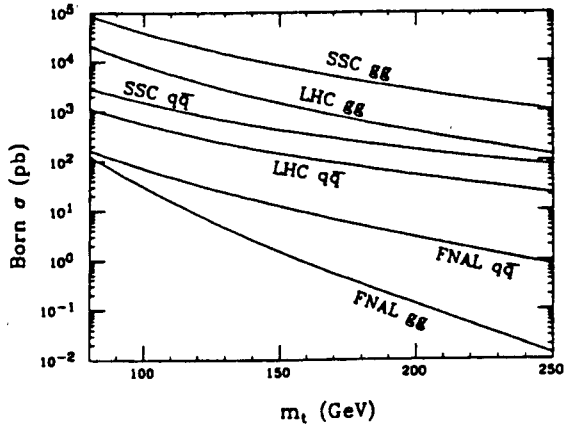

Figure 29: The Born cross sections for glue-glue and quark-antiquark processes at SSC, LHC, and Tevatron.

the machine, so small x parton distributions are more important.[27] The overall uncertainty due to structure functions is 20%, and the scale uncertainty is 20%.

In order for experiments to set lower limits on the mass of the top quark, it is important to have good central values for the production cross sections as well as estimates of the systematic errors. A study of this type has been done by R. Ellis[28]. To evaluated the possible systematic errors in the theoretical cross section, the Λ parameter is varied between 60 and 250 MeV, and the scale parameter is varied between half the mass of the top to twice the mass of the top. Two different parton distribution parameterizations are used; DFLM[29] and HMRS[30]. This re-analysis of the cross section leads to slightly larger top production cross sections than were used previously. Much of the remaining uncertainty can be attributed to structure function differences as shown in Figure 30. The more recent HMRS structure functions increase the production cross section at high mass relative to the DFLM structure functions. The resulting range of values for the top production cross section as a function of the top mass are shown in Figure 31 where the upper and lower bands correspond to the range of allowed

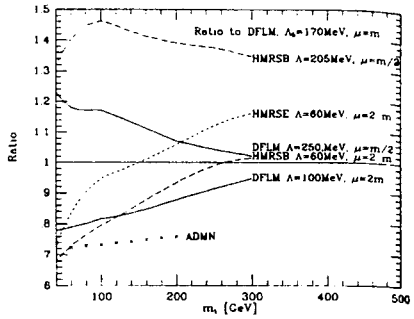

Figure 30: Ratio of extreme values to DFLM central values.

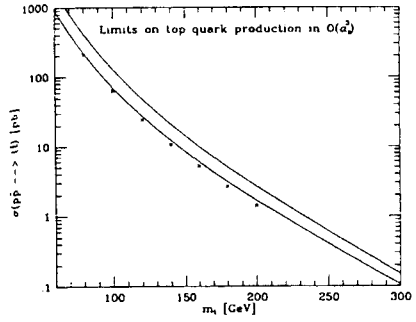

Figure 31: Upper and lower limits on top quark production.

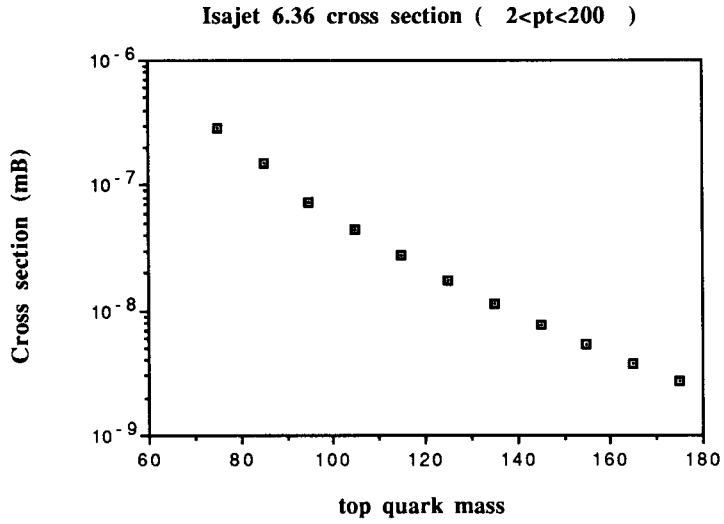

Figure 32: Isajet cross section for top production.

values. This analysis is extremely useful to experimentalists since it reduces much of the uncertainty in estimating the errors on the theoretical cross sections used to calculate limits. The Isajet Monte Carlo which is often used for experimental studies has a central value for the top cross section which compares well with the theoretical values (see Figure 32).

W Gluon Fusion

As the top quark mass increases, the quark-antiquark production mechanisms begin to dominate over the glue-glue mechanisms. The requirement of producing a top and an anti-top quark reduces the cross section rapidly for heavy masses. The diagram for the W gluon fusion mechanism shown in Figure 33 requires the production of only a single top quark, the cross section can be larger than the pair production cross section for some masses. The normal cuts used for selecting top quark candidates

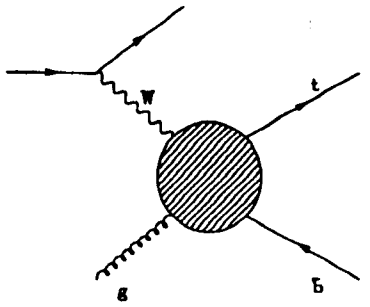

Figure 33: W gluon fusion diagram.

reduce the signal from W gluon fusion because the b jet which accompanies the top tends to have smaller p_t and larger rapidity than the average jet in the pair mechanism. Because backgrounds are large both at low p_t and at larger rapidities, the cuts used usually discriminate against these regions. Before cuts, the W gluon fusion process is larger than the pair process for top masses greater than 190 GeV at the Tevatron (see Figure 34). In order to enhance the top signal above the QCD and W plus jet backgrounds, it is assumed that one jet can be tagged as a b jet. When two jets are required in the final state, the signal from W gluon fusion is below the background from W plus jet production. For the three jet case, the background situation is better as shown in Figure 35, but the W gluon process is small for most top masses because it does not normally produce a large jet multiplicity. Even with these problems, it is worthwhile to attempt to find a strategy which would yield a sample of tops from this process, because the tops are 100% polarized. Isolation of such a sample would be an extremely useful tool in studying the properties of the top quark.

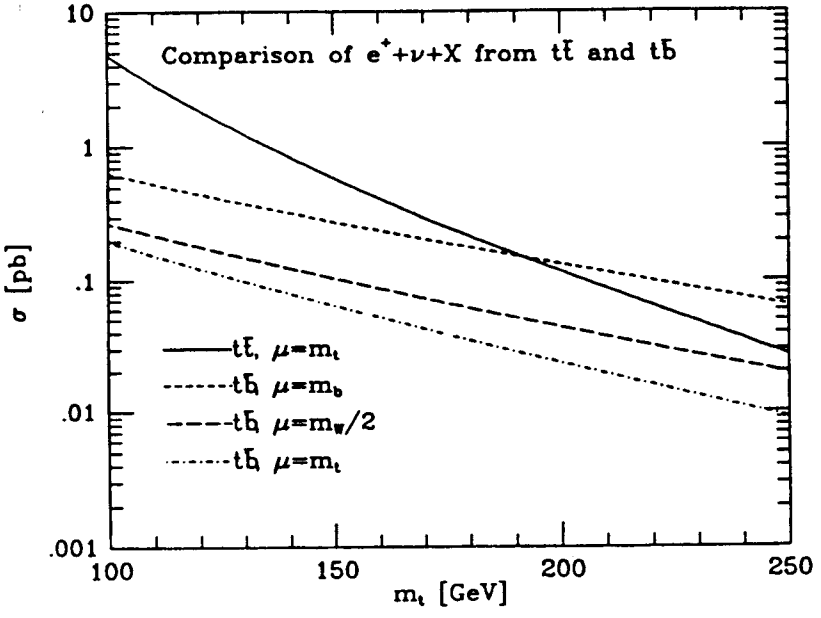

Figure 34: Comparison of the electron neutrino and jets production from $t\bar{t}$ and $t\bar{b}$ production at tree level.

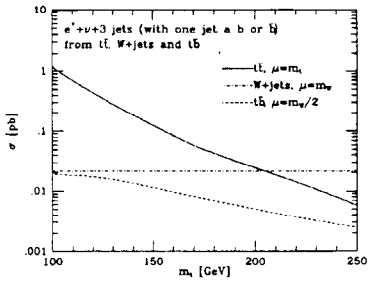

Figure 35: Comparison of rates for electrons, missing E_t, and three jets from various sources.

Top at the LHC and SSC

Cavanna et al.[31] have summarized a study of top quark production for the LHC. The study assumes an η coverage of 1.5–2.0 with a 0.1 by 0.1 granularity. The trigger is assumed to be fully efficient for e's and μ's above 30 GeV with muon identification extending down to 10 GeV in p_t for an η less than 2.5. One object of the study was to try to avoid using $\not\!\!E_T$ in the analysis. At least one reason for this is the difficulty in making good $\not\!\!E_T$ measurements in an environment where there are several interactions per crossing. This effect (which is quite a bit more important for the LHC than the SSC) comes about because fluctuations in the energy deposited by the minimum bias events cause large uncertainties in the missing E_t. The study uses both the Isajet Monte Carlo which is a parton evolution plus cascade type model, and the Eurojet Monte Carlo which uses matrix elements in next to leading order. The results of the study are shown in Figure 36. Note that for a 200 GeV top quark, which due to the small production cross section at the Tevatron for this mass would be an excellent opportunity for the SSC or LHC, the background $b\bar{b}$ process has a cross section six orders of magnitude larger than the signal. Fortunately, the p_t spectra of the two processes are very distinct as shown in Figure 37. To further separate the top events from the background, the lepton is required to be isolated. In massive quark decay (either b or t), the lepton has a maximum p_t of m/2 relative to the decay axis. Hence this p_t of the

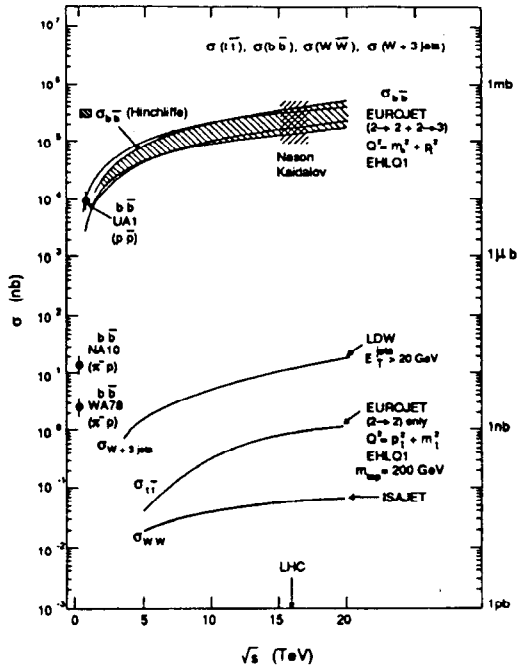

Figure 36: $t\bar{t}$ cross section and the major backgrounds as a function of the cm energy.

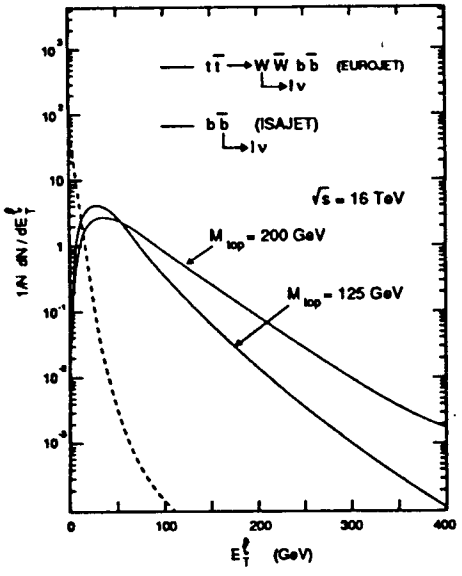

Figure 37: E_t distributions of lepton sources.

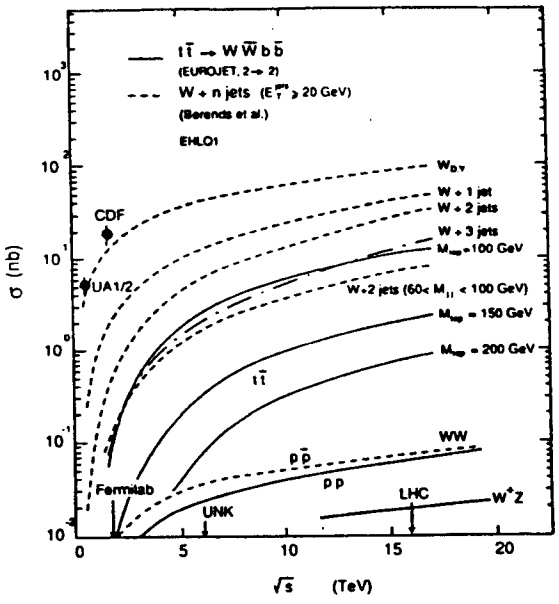

Figure 38: $t\bar{t}$ signal and background processes as a function of cm energy.

lepton is much greater in t events leading to leptons which on average are better separated from their parent jet. There is some inefficiency in this type of cut since the lepton may overlap with another jet, or may fail the cut due to the buildup of nearby minimum bias event energy. The cut required is a few GeV in a cone of radius 0.1. A larger cone radius and/or a smaller energy requirement can be made at the SSC where the number of interactions per bunch crossing is smaller.

If the top quark mass is about 150 GeV, then the SSC/LHC become top quark factories, producing of order 10^6 to 10^7 events per year. The primary production mechanism would be low x glue-glue processes and the principle background would be W plus jet production as indicated by the energy dependence of the cross sections shown in Figure 38.

The extremely large number of produced events allows for special cuts to be

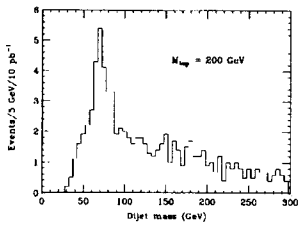

Figure 39: Dijet invariant mass for $t\bar{t}$ events with mass 200 GeV. The dijet system has $p_t > 60$ GeV, an isolated electron above 20 GeV, missing E_t greater than 20 GeV, at least three jets, and two tagged b jets neither of which is used in the dijet system.

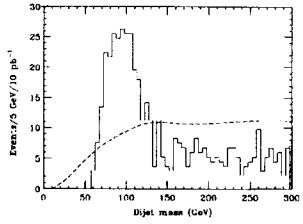

Figure 40: Dijet invariant mass for the two highest energy jets with dijet p_t greater than 180 GeV when the top mass is 150 GeV. The dashed curve is the W plus jets background.

made in studying the top mass. Strict cuts which improve the mass resolution can be used to advantage.[32] The technique requires very high p_t cuts on each jet to improve the energy resolution of the hadron calorimeter, a high p_t cut on a reconstructed W to reduce W plus jet backgrounds, and a smaller than normal jet cone to prevent merging of jets from the high p_t W's. Combinatorial backgrounds can be reduced by tagging b jets and eliminating these jets from combinations used to reconstruct the W's. The top mass is measured by forming the invariant mass of a tagged b jet with a W. The invariant mass distributions are shown in Figures 39–41. The resulting systematic error on the top mass (which comes primarily from uncertainties in the jet scale corrections) is estimated to be 3 GeV.[33]

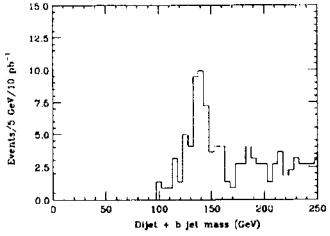

Figure 41: Top reconstruction from a dijet with p_t above 180 GeV and a tagged b jet. The dijet is required to have invariant mass less than 110 GeV consistent with a W.

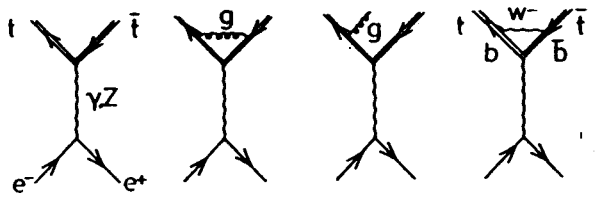

Figure 42: Radiative corrections for top production in e^+e^-.

Top Quark Production in e^+e^-Colliders

The cross section for production of a pair of top quarks at an e^+e^-collider is

$$\sigma = \frac{3-\beta^2}{2}\beta\sigma^{VV} + \beta^3\sigma^{AA}$$

where the vector-vector and axial-axial cross sections are

$$\sigma^{VV} = \frac{4\pi\alpha^2(s)}{s}e_e^2e_t^2 + \frac{G_F\alpha(s)}{\sqrt{2}}e_ev_ev_t\frac{m_Z^2}{s-m_Z^2} + \frac{G_F^2}{32\pi}\left(v_e^2+a_e^2\right)v_t^2\frac{m_Z^4 s}{(s-m_Z^2)^2}$$

$$\sigma^{AA} = \frac{G_F^2}{32\pi}\left(v_e^2+a_e^2\right)a_t^2\frac{m_Z^4 s}{(s-m_Z^2)^2}\ ;$$

and the vector and axial charges are

$$v_f = 2I_3^f - 4e_f sin^2\theta_W$$

$$a_f = 2I_3^f \quad .$$

The value of α at the scale of the Z is approximately 1/127 rather than the low energy value of 1/137, and the radiative correction diagrams are shown in Figure 42. For a top quark of about 150 GeV, the maximum cross section will occur about 30 GeV above the threshold value of twice the top mass. The magnitude of the cross section is smaller than that at proton machines because the top quarks are not produced by the strong cross section. Assuming a machine running at 2 10^{33} (about four times the current record for e^+e^-machines) for one year (10^7 seconds), the number of produced events would be 20,000. Thus the e^+e^-machines are unlikely to be top factories, and one should look for things

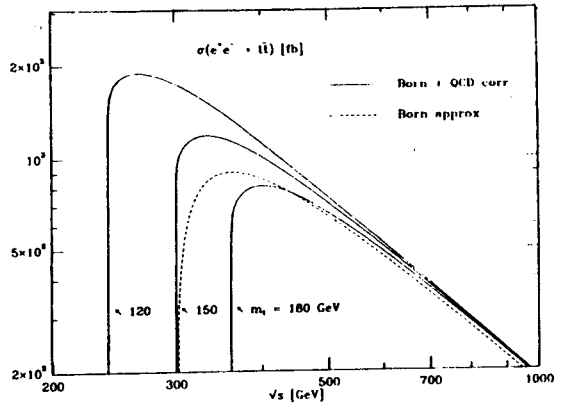

Figure 43: The e^+e^-cross section for top production including QCD corrections.

to do which require precision and which are not statistically limited. As in the hadron case, the peak production cross section decreases rapidly with increasing top mass (see Figure 43). The two photon mechanism for top production will also produce events at a rate one to two orders of magnitude smaller.[34] In these events (which therefore occur at a 1-10% rate), there is no center of mass constraint due to missing momentum along the beam line in analogy to the normal case in hadron machines.

Example Machine

Since there will be several talks at this Institute about designs of linear colliders from SLAC, I have decided to use the DESY 500 GeV design[35] as an example of the type of machine that people are considering for this physics. I found the basic thesis of this design rather interesting for SLAC since it argues that conventional S band technology (of which SLAC is an example) extrapolated to the 500 GeV energy range is the best technology. The design argues that most of the "new" ideas for linac designs have been found, on further study, to be impractical because of low efficiency in providing large enough accelerating gradients at reasonable

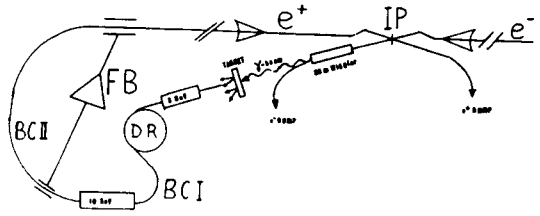

Figure 44: DESY design reuses the electron bunch for positron production.

power consumption levels. Higher frequencies (than S band) would require some additional technical development. The higher frequency also has a lower total stored energy since this is proportional to the transverse cavity size which is smaller. This lower stored energy makes beam loading a greater problem. The smaller physical dimensions of the cavities for higher frequency linacs require proportionally tighter tolerances on construction and assembly. All-in-all, the conclusion of this study is that perhaps one should use the standard frequency.

In any machine of this type, positron generation is a major technical challenge. Given the difficulty of generating high energy positron beams of high intensity and small phase space, some emphasis needs to be placed on what to do with the positrons after the collision with the electron bunch. As you may know, in the SLC, the positrons are discarded in a beam dump. Conserving the positrons in some manner might be very useful. One example of these types of investigations[36] is shown in Figure 44. Here the positrons themselves are not saved, but the spent electron beam is used on a target for positron production.

A significant problem for machines of this type, which are quite long, but require excellent stability, is the issue of ground vibration. Long term measurements of the ground noise in the HERA tunnel indicate noise at the 100 nm level in the frequency range of interest. The effect on the beam is enhanced by $2\sqrt{N}$ where N is the number of quads (which would be 1000 in the DESY design). The data (shown in Figure 45) show some interesting features. The dashed line in the figure is the desired tolerance for 500 GeV operation, and since it is not too far

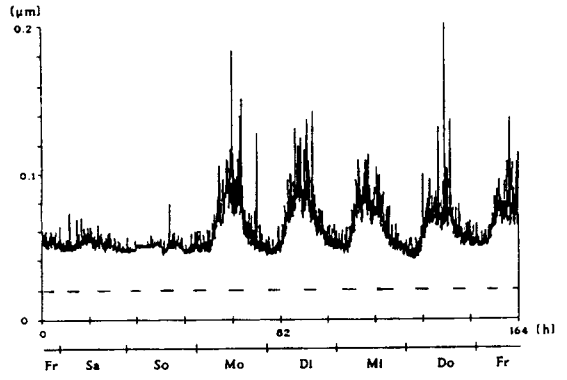

Figure 45: Measurements of ground noise in the HERA tunnel during one week. Broken line represents the machine design tolerance.

Energy	300-500 GeV
Luminosity	2 10^{33}
Klystron Power	100-150 MW
Klystron Efficiency	45%
Bunches	172
Bunch Separation	3.2 m
β_x, β_y	3mm, 0.3mm
Beam Size	169 x 5 nanometers
Length	30 kilometers

Table 2: Parameters for and Example Linac taken from the DESY Design

below what is observed, suggests that noise isolation techniques for the machine elements might suffice. Note that the weekends are significantly quieter! The rough parameters for the DESY design are shown in Table 2.

Top Measurements at e^+e^- Colliders

The Top Mass

Once the top quark mass is known, e^+e^- linear colliders could play an important role in investigating some of the properties. For example, it is possible to achieve

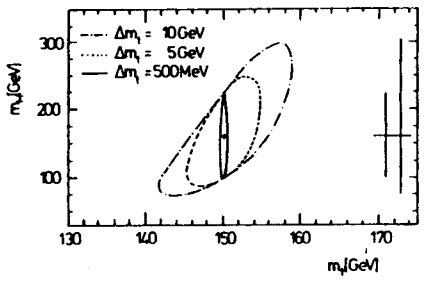

Figure 46: Constraints on the Higgs mass for a central value of 150 GeV using LEP, the mass of the W, and e^+e^- polarization asymmetries.

an accuracy of approximately 500 MeV on the mass of the top.[37] Recall that the measurements at hadron colliders may be limited to a few GeV unless systematic errors on the jet scales can be eliminated. This measurement is made by using the threshold behavior of the top production cross section. It requires high statistics measurements at several points along the threshold curve together with accurate theoretical calculations including effects of the finite width of the top. The main thing which one learns from such a high accuracy measurement of the top mass is an increase in the accuracy of the predicted Higgs mass (see Figure 46) within the Standard Model. Of course, if the Higgs has been independently detected, the mass can be compared to the calculated value in the hopes of finding non-standard model physics.

Other "Top"-ics

QCD studies of the region around the top threshold are interesting because the very heavy mass of the t quark improves the predictions of QCD perturbation theory. A quick calculation shows that the Bohr radius for a 1S toponium state is (don't forget color factors)

$$a_0 = \left(\frac{2}{3} m_t \alpha_s\right)^{-1} .$$

For t quark masses greater than 130 GeV, the lifetime of the t is too short for one complete revolution in this orbit, so the state hardly exists.[38] Thus there

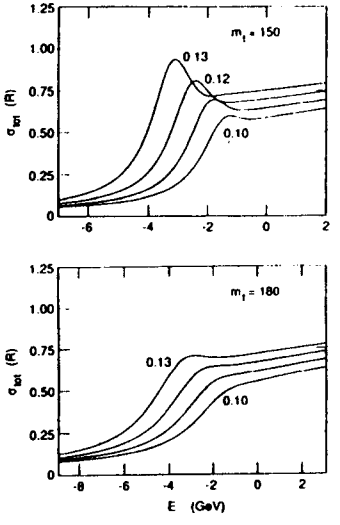

Figure 47: Excitation curves for t quarks near threshold. The labels indicate the value assumed for α_s at the Z mass.

is no ground state. In addition, the width of the toponium state is larger than the 1S-2S level spacing. The lineshape expected in this complicated region has been solved numerically[41] for the QCD potential and is shown in Figure 47. The heavy mass of the top also helps suppress gluon radiation along the direction of the top.

Light Higgs radiation from t quark pairs or perhaps the t decays of heavy Higgs provide an opportunity to measure the Higgs to top quark Yukawa coupling. This would be quite interesting, unfortunately the cross sections are probably small (10 fb) or (10*−36). The expected value for this coupling in the Standard Model is

$$g^2_{ttH} = \sqrt{2} G_F m_t^2 .$$

The diagrams for the relevant light Higgs processes are shown in Figure 48. For an integrated luminosity of 20 inverse femtobarns, one would obtain 100 such events for Higgs masses of order 60 GeV and 20 events for masses of order 120 GeV (see Figure 49).

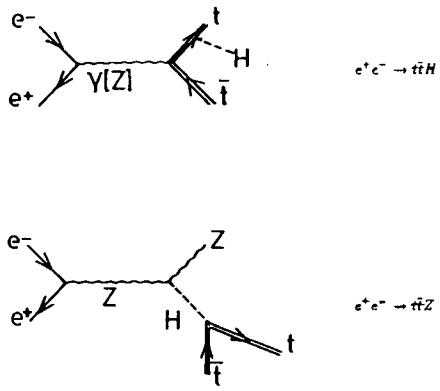

Figure 48: Light Higgs radiation from t quarks.

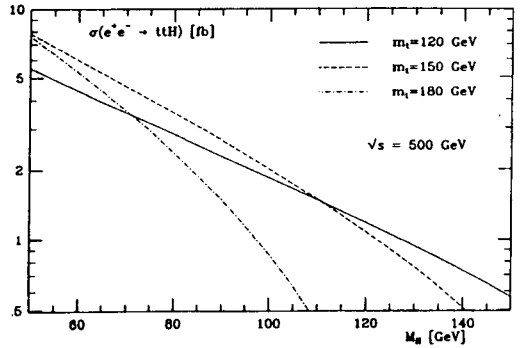

Figure 49: The e^+e^-cross section for $t\bar{t}$ H production at 500 GeV cm energy as a function of the Higgs mass for three top masses.

If the Higgs is heavy (greater than 2 mtop), then HZ production with subsequent Higgs decay to $t\bar{t}$ will contribute to the $t\bar{t}$ cross section. For a top mass of 100 GeV, the $Zt\bar{t}$ cross section increases by almost a factor of two when the Higgs mass is about 250 GeV.[42] The Z momentum spectrum should be useful in separating the two-body HZ final states from the $Zt\bar{t}$ states.

In addition, the ability to cleanly tag a top quark in an event with top pair production may provide the ability to look for rare decays of the top quark. A word of caution is probably in order on the subject of rare decays of the top quark however.[39] The rare decays of the strange quark have been the subject of many experiments and theoretical papers as have the rare decays of the b. The same cannot be said for the c quark and by extension, probably even more so for the t. The fundamental difference is that the Cabbibo suppression of s decays allows the K meson systems to have long enough lifetimes to have interesting rare decays. The c on the other hand decays quickly to an s. In the same way, b decays are likely to be interesting, but the same rapid decay mechanism coupled with the very large mass of the t, and its consequently very short lifetime, probably suppress most "rare" t decays below detectable levels.

Other Physics

New gauge bosons would provide a rather spectacular signature for new physics at an e^+e^-collider. Figure 50 shows the signal[40] in muon pairs from a 750 GeV Z′ with the solid curve giving the Born approximation and the dashed curve the shape with QED corrections. The absolute magnitude of the cross section is a factor of 3000 smaller than the values currently being used at LEP which requires correspondingly large increases in the design luminosity of the machine. Note that in Figure 50, for a luminosity of 10^{33}, the scale would be in events per second. Projected luminosities for most new machines are in the 10^{33} range which as shown in Figure 51 is necessary to have sufficient rates for standard physics at these energies.

In searches for rare new physics, it should be pointed out that at higher energies, there are some new challenges. The logarithmically rising two-photon cross section becomes no longer totally negligible. A cut is required on the total ob-

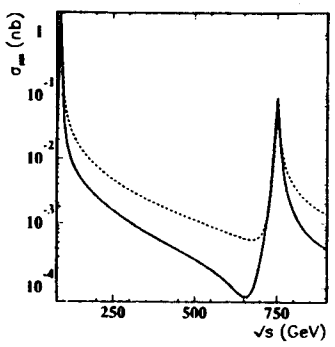

Figure 50: The total cross section for muon pair production as a function of cm energy in the presence of a Z′ of mass 750 GeV. Born approximation (solid), QED corrected (dashed).

served energy which means that event signatures which involve neutrinos may not always be useful. While one would think perhaps to use missing transverse energy (which as in proton collisions is small for the two photon events), this will not eliminate a further background which becomes important at these energies, namely WW production. As shown in Figure 52, these events can contribute significantly unless a cut is made on $\Delta = 1 - \frac{s'}{s}$ where s′ is calculated from the observed energy and s from the nominal cm energy.

Charged Higgs

In the Standard Model, the only Higgs particle is neutral, but charged Higgs particles do exist in extensions of the Standard Model where there are two Higgs doublets. These extensions are partially motivated by supersymmetry which requires a doubling of the Higgs sector to provide masses for up and down type fermions. In the minimal supersymmetric extension, the masses of the charged Higgs are expected to be heavier than the W. A parameter $tan\beta$ is the ratio of the vacuum expectation values of the Higgs fields which give masses to the up and

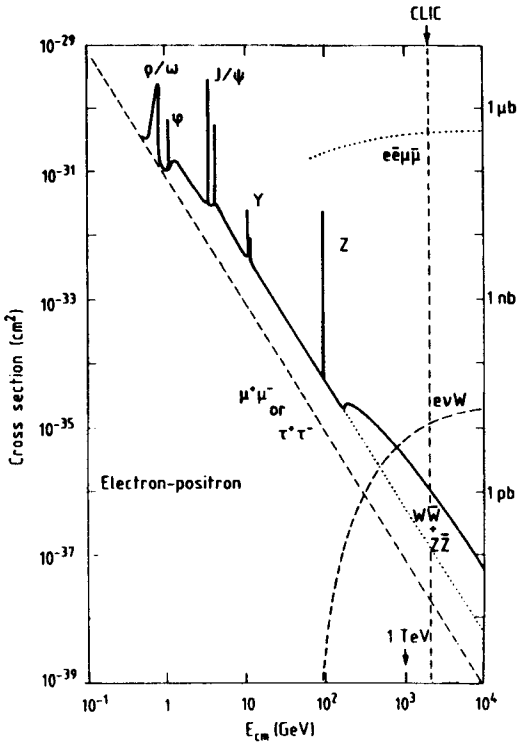

Figure 51: e^+e^- cross section as a function of cm energy. Point cross section (dashed).

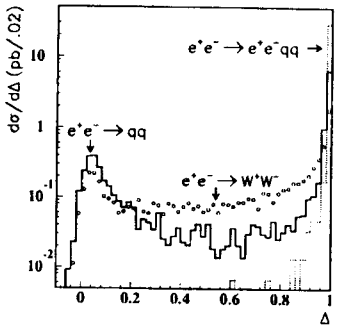

Figure 52: Final state energy spectrum for an e^+e^-collider with cm energy 500 GeV. Beamstrahlung effects are not included.

down type fermions. Theoretical prejudice for the value of the parameter is

$$1 \leq \tan\beta = \frac{v_2}{v_1} \leq \frac{m_t}{m_b} \sim 30 \; .$$

The charged Higgs phenomenology is very important for the study of the top because it is possible that the top has not been seen due to charged Higgs decay modes. If the top is heavier than the mass of the charged Higgs plus the mass of the b, then for some regions of $tan\beta$, the top decays can be difficult to observe. For this scenario, we need to find a region of $tan\beta$ where the normal t decay mode to the W is small. Figure 53 shows the charged Higgs decay modes as a function of $tan\beta$. Note that either large $tan\beta$ or small $tan\beta$ would suppress the usual W modes. If $tan\beta$ were small, the top decays would still be found because the dominant charged Higgs decay mode is then two jet. Semileptonic decays of the b would still provide isolated leptons at reduced rates. For large $tan\beta$ however, the tau decays of the Higgs would dominate. In this case, the standard decay signatures for the top would have low efficiency. The clue to this scenario would be a breakdown of e, μ, τ universality.

Roy et al.[43] have tried to enhance the charged Higgs signal above the W background in heavy top decays at the LHC, and they conclude that it should be possible to see this decay if the charged Higgs is at least 20 GeV heavier than the

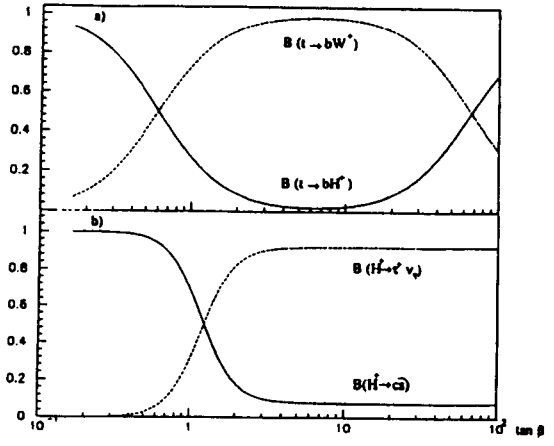

Figure 53: Branching ratios for 200 GeV top mass and 130 GeV Higgs mass.

top. The signal comes from

$$t \rightarrow bH^+$$

while the background comes from

$$t \rightarrow bW^+ \; .$$

The two possible Higgs decays are cs and $\tau\nu$ with branching ratios depending on $tan\beta$. Since there are two tops to decay, there are several possible final states.

$\tau\tau$

For two tau final states (primarily large $tan\beta$), the cuts used were a 10 GeV jet (from τ decay), at least 20 GeV missing p_t, and an isolation cut on the τ. This channel gives the best signal to background ratio because it detects both HH and HW events. It is not possible to reconstruct the W in the latter sample due to the large number of missing neutrinos. The WW background (see Figure 54) normally has at least two hard jets, while the signal has at least one soft jet so that some

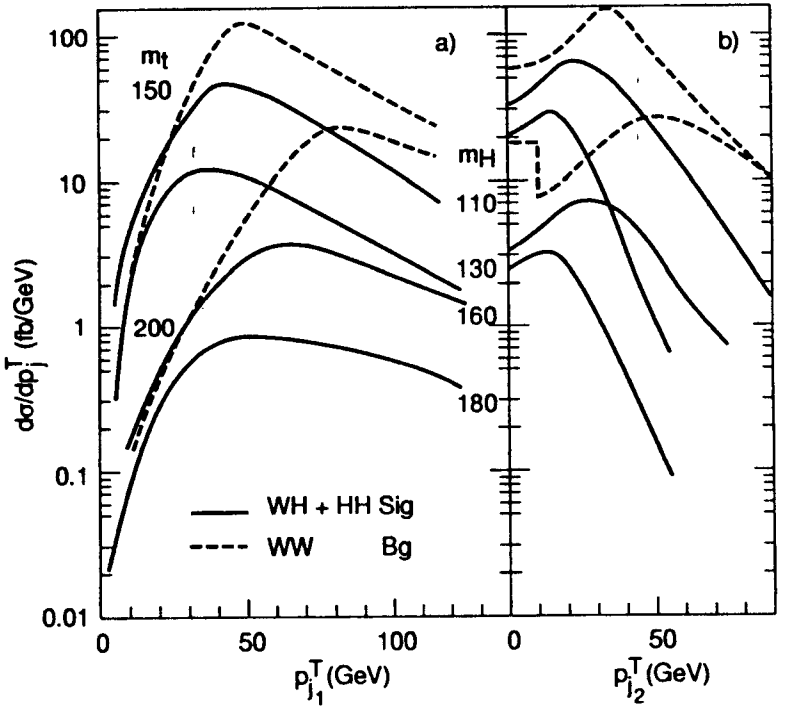

Figure 54: Signal and background from HH, HW, and WW events.

additional rejection of the background can be achieved by requiring that there be no b jet with p_t greater than 30 GeV.

Other detection modes include final states with one detected τ and either a hard or soft muon. The signal for the hard muon case comes primarily from WH production. In the soft muon case, the muon comes primarily from the decay of the H, and the background from the soft tail of the W decay. Also as in the case of standard top decays, it is possible to look for multijet signatures, for example, a τ and several jets. The τ decay comes from the H decay, and the jets either from an H or a W. The major disadvantage of this mode is the large background from W + jets. The advantage is that since there are fewer missing neutrinos, you can reconstruct the transverse mass of the W or H and look for events in the high mass tail beyond the kinematic limit for W's (see Figure 55). (Actually the background in this tail is a combination of measurement errors and high p_t W's.)

Experimental Charged Higgs Searches

For a charged Higgs lighter than the top, the decay $t \rightarrow bH^+$ could represent the major decay mode of the top and depending on the decay signatures of the Higgs, the top could evade normal experimental searches. For this reason it is necessary to design a search strategy specific to this decay. The UA1 collaboration[44] used both single muon plus jets and dimuon signatures for this search. This is similar to the standard top search except that the muon from τ decay is softer than that from the standard decay chain. For the μ + jets mode, the jets must have E_t greater than 7 GeV and be accompanied by an isolated μ with p_t greater than 8 GeV. The transverse mass of the event must be less than 60 GeV. There are 298 candidate events which are analyzed with a cut on a Higgs likelihood function which compares signal and background distributions in missing E_t, muon p_t, and the angle between the second highest jet and the beam axis in the rest frame of the four body system consisting of the muon, the two jets and the missing E_t.

The dimuon search[45] requires two muons with p_t greater than 6 and 3 GeV with isolation requirements only on the first muon. The dimuon invariant mass is required to lie between 6 and 50 GeV, and there must be at least one central jet

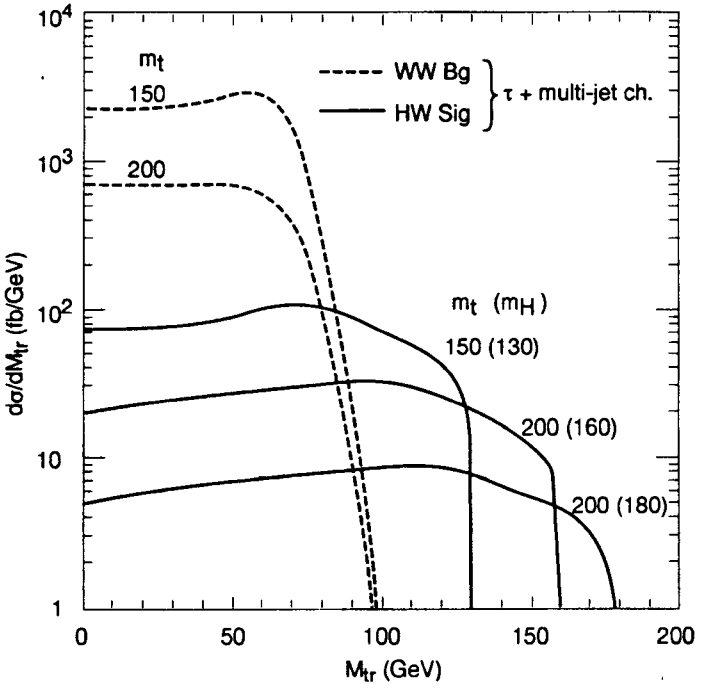

Figure 55: Signal and background for the τ + multijet search.

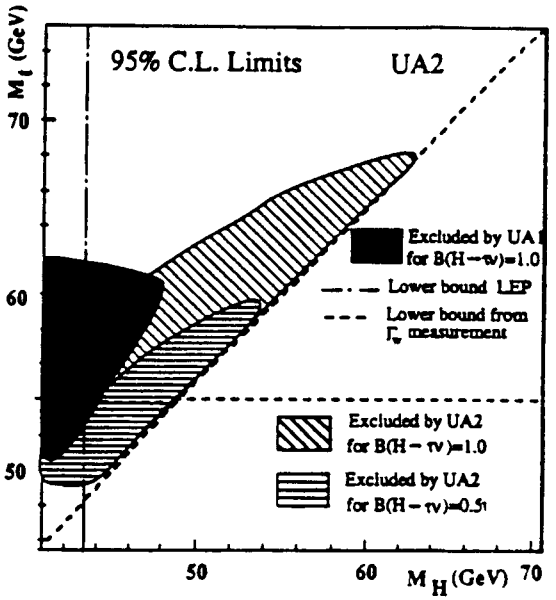

Figure 56: Regions of the top mass vs. charged Higgs mass plane excluded by UA1 and UA2.

with E_t greater than 10 GeV. Cuts are made on the angle between the jet and the muon as well as on the angle between the jet and the beam. A likelihood function is constructed as in the muon + jet search which involves the p_t of the first muon and its isolation. The combined results from UA1 of the two search methods are shown in Figure 56 along with the UA2 results discussed below.

A search for the same process by the UA2 collaboration[46] looks for events with electrons or taus accompanied by large missing E_t. The number of events found which contain electrons is used to find the W background contribution. An excess of τ's would signal the presence of Higgs production. The event $\not{E}_T$ must be greater than 20 GeV. As shown in Figure 57, this cut preserves reasonable efficiency for the charged Higgs even though the spectrum is softer for the signal than the background. The leading jet in the event is required to have at least

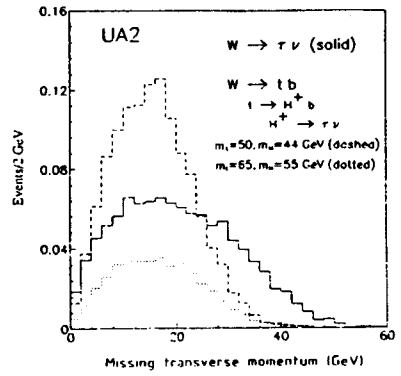

Figure 57: p_t distributions for signal and background in the UA2 charged Higgs search.

17 GeV p_t, and there can be no opposite jet in ϕ with E_t greater than 10 GeV (to eliminate QCD backgrounds).

The most interesting part of this analysis is the method used to separate the τ sample. The first of two cuts is based on a variable called hadronicity

$$\xi = \frac{\text{hadronic energy}}{\text{total}} .$$

The hadronicity is required to be in the range $0.01 < \xi < 0.90$ so that there is some hadronic energy and some electromagnetic energy. There can only be one charged track in a 10 degree cone around the energy deposited in the calorimeter. This fits the hypothesis of a one prong tau decay (one charged pion accompanied by several pi-zeros). The second major cut for the tau sample is called the profile cut. The profile ρ is defined as

$$\rho = \frac{\mathrm{Em} + \mathrm{Em}'}{\mathrm{E_{tot}}}$$

where Em and Em′ are the leading and neighboring cell energies for the energy cluster. The profile is required to be less than 0.75 which requires that the cluster be tight, i.e., consistent with the low invariant mass of a τ candidate. Figure 56 shows the results of the UA2 search.

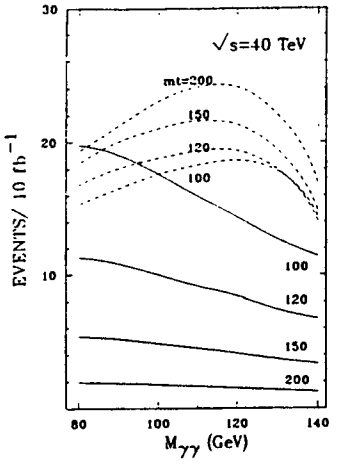

Figure 58: Expected number of $t\bar{t}$ $\gamma\gamma$ events at the SSC in one year from prompt photons (solid), and Higgs production (dashed).

Top Backgrounds for Higgs Searches at SSC/LHC

For the SSC or LHC, one of the more attractive modes for neutral Higgs searches is the $\gamma\gamma$ decay mode. For Higgs masses up to 80 GeV, the Higgs would probably be already found at LEP, and for masses above 140 GeV, the four lepton final state from $H \rightarrow ZZ$ is probably most useful. But in the intermediate mass range, the $\gamma\gamma$ mode is best. Most studies of the backgrounds for this search have concentrated on the general QCD backgrounds and the backgrounds from radiated photons from light quarks. But it is also possible[47] for prompt photons produced along with $t\bar{t}$ pairs to represent a significant background in the low mass (< 100) range. The relative magnitudes of the two cross sections at the SSC are shown in Figure 58.

Top Polarization

The Higgs coupling to a fermion is proportional to the mass of the fermion. Thus the Higgs coupling to the top increases with top mass. Since the longitudinal

component of the W can be identified with the Higgs field, the longitudinal coupling of the top increases with mass but the transverse coupling does not. Thus for heavy top, the longitudinal coupling can become large.[48] The polarization can be measured by looking at the decay distributions in the W rest frame with respect to the W direction in the t rest frame. The longitudinal and transverse distributions in this frame are

$$\frac{d\Gamma}{d\cos\theta_w} \sim \left\{ \begin{array}{c} sin^2\theta_w \\ (1 \pm cos\theta_w)^2 \end{array} \right\} .$$

The polarization of the top quark is preserved in the decay and results in a polarized W. For heavy top, the b quark in the decay is left-handed and therefore a W emitted parallel to the direction of the t polarization must be longitudinal. Leptons from the decay of the W will be emitted preferentially parallel to the t spin direction while emission in the opposite direction is forbidden.[49] Top polarization is large in the W-gluon fusion process, and the analysis of the polarization from either this process or the normal $t\bar{t}$ production will yield further information about the top quark couplings.[50]

Top Quark Fragmentation

The width of the top quark scales with mass as

$$\Gamma \sim 0.17\mathrm{GeV}(m_t/m_W)^3$$

and the lifetime is $\tau = 1/\Gamma$. Thus if the top quark is heavy enough, the width becomes large (see Figure 59), the lifetime is very short, and there is insufficient time for the top quark to fragment before it decays. If the top quark is light however, there is time for the usual fragmentation process. This situation may lead to changes in the t quark z fraction distribution as well as the distribution of radiated gluons in the fragmentation process.[51]

The fragmentation spectrum of mesons is known to become more strongly peaked near z=1 for heavier quarks. This is a consequence of momentum conservation in the decay of the Qq system.[52] One way to look at the z spectrum is to estimate the amount of energy radiated in the form of soft infrared gluon

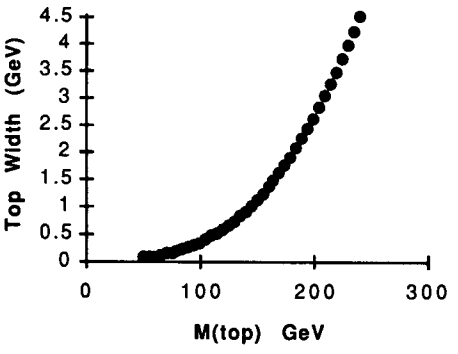

Figure 59: Predicted top width as a function of the top mass.

radiation in the fragmentation process. This energy loss is approximately

$$\Delta E = \frac{\kappa \gamma h}{2\pi \Gamma_t}$$

where $\kappa = 1$ GeV/fm is the fragmentation string constant. This approximation gives an energy loss due to fragmentation of about 5 GeV for a 100 GeV top at cm energy of 500 GeV. For a leading log calculation of these effects, see Dokshitzer, Khoze and Troyan.[53]

The string fragmentation picture of this effect is that if the quark lifetime is short, the t and $\bar{t}$ do not separate far enough to stretch the string in the lifetime of the t quark. The flight path of the quark is $\gamma\tau$ which will be less than 1/2 fermi when

$$E < \frac{1}{2}\frac{m_t^4}{m_w^3}$$

The color string is stretched between the $b\bar{b}$ pair after the decay. Interestingly, the direction of this stretch is not the same direction as the initial $t\bar{t}$ direction. One might see a multiplicity enhancement in the $b\bar{b}$ hemisphere[54], but it looks like a difficult measurement. In the study, hard non-colinear gluon radiation as well as beamstrahlung and bremsstrahlung have been neglected. The effect is significantly reduced by hard gluon radiation which may need to be removed with event shape requirements. Also, fragments from the b quark decays need to be removed to

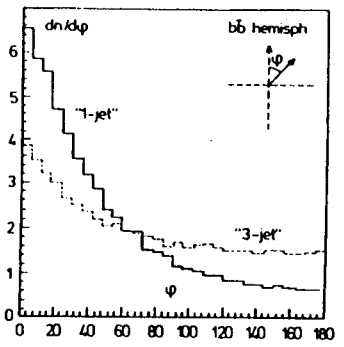

Figure 60: Distribution of the azimuthal distribution of particles with rapidity less than 1 and with B decay products removed. The solid curve represents production from the $b\bar{b}$ flux tube while the dashed curve comes from events where the color flux tube is also stretched by t decay products.

make the signature visible. This assumes a good microvertex detector to separate these products with high efficiency. The effect is diminished by inefficiencies in this device but not eliminated. One must also distinguish between one and three jet topologies. The one jet topology is the one where both tops decay immediately and there is only one string direction. The three jet topology occurs when there is some non-negligible initial state radiation from the top (see Figure 60).

Supersymmetric Top

The Minimal Supersymmetric Standard Model (MSSM) allows the supersymmetric top (stop) to be much lighter than the top and other squarks. It is also possible for the stop in particular to evade the current bounds set on squark production by the CDF squark searches. The MSSM parameters are shown in Table 3.

top mass	$100 < M_t < 200$ as in SM
charged Higgs	> 40 (LEP)
charged Higgs	$M_{H+} > M_W$
s-glue	$M > 132$
s-b	> 45 (LEP)
s-t	> 45 (LEP)

Table 3: Nominal parameters for the Minimal Supersymmetric Standard Model.

Decay modes for the heavy to light stop include:

$$t \rightarrow bW^+$$
$$t \rightarrow \tilde{t}_1 \tilde{z}_k$$
$$t \rightarrow \tilde{b} \tilde{w}_k^+$$
$$t \rightarrow \tilde{t}_1 \tilde{g}$$
$$t \rightarrow H^+ b\,.$$

Generally, the introduction of the stop leads to harder $\not\!\!E_T$ spectra for events but softer leptons and jets. In addition, the Standard Model always involves W decay, but the MSSM does not.

An analysis by Krasnikiv et al.[55] indicates that the mass of the Higgs together with that of the top can distinguish between the Standard Model and the SUSY extension when the top mass is greater than 150 GeV. Shown in Figure 61 are four different regions in which the top and Higgs masses might be found. Region II would exclude both the SM and the MSSM. Region IV does not distinguish between the two models, but I is allowed only in the SM and region III is allowed only in the SUSY extension.

The CDF collaboration squark search limits are m(squark) > 170 GeV for super-glue or gluinos less massive than 400 GeV and the limit on the gluino is m > 150 GeV. These limits are based primarily on the search for events with missing E_t. The limits assume that all 12 types of squarks (six flavors x R, L) are degenerate in mass. Hence if only the stop is light, the assumed production rate would be decreased by a factor of twelve. The search also assumes direct decay of the squark to the lightest supersymmetric particle (LSP) rather than the more likely cascade of decays between various super-particles. This cascade decay softens the $\not\!\!E_T$ spectrum, and reduces the limits by about 30 GeV. Nevertheless, this is an important topic and further work is needed on these limits because for

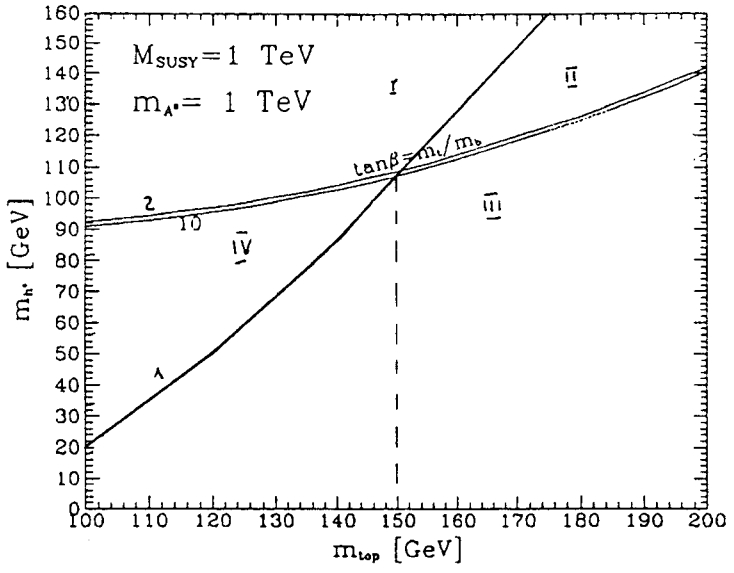

Figure 61: Four regions in the Higgs and top mass plane. Region I is allowed only in the Standard Model (SM), Region II excludes both SM and MSSM, Region III is allowed only in the MSSM, and Region IV does not distinguish between the models.

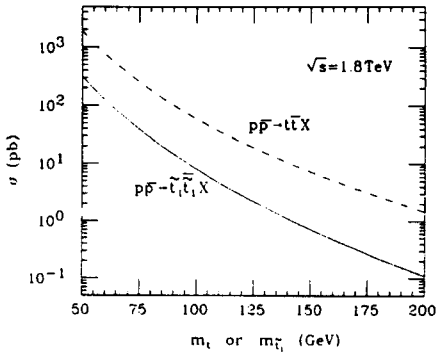

Figure 62: Top and stop production at the Tevatron.

heavy top, there may be only a single light squark eigenstate, and the SM decays on which most lepton searches for the top rely, becomes a small branching ratio. The dominant decay is

$$t \to \tilde{t}\tilde{Z} .$$

The stop should be heavier than the LEP bound of 45 GeV, and if the top were moderately light and/or the LSP were heavy, these decays could be somewhat suppressed. Otherwise, with a sufficiently light stop, which is produced in pairs by the strong interactions in $p\bar{p}$ (see Figure 62), it may be possible to find a signature for these decays in the $\not{E}_T$ spectrum.[56]

Top Quark Condensates

Within a model where the top quark is heavy, it is possible to think about forming a scalar state from the $t\bar{t}$ system. Suppose in addition, that the Higgs particle as a fundamental scalar does not exist, but that its role of mass generation in the Standard Model is played by this "dynamical" top quark condensate.[57] In this scenario, the Higgs mass is certainly related to the top mass. This theory leads to testable predictions by requiring a low energy effective Lagrangian which looks like the Standard Model. By matching the low energy behavior of the theory to

the SM, there are new constraints on the theory which predict

$$M_{top} \approx 230 \text{ GeV} ,$$
$$M_{Higgs} \approx 260 \text{ GeV} .$$

These predictions are claimed to be relatively insensitive to the assumed values of the coupling constant at the compositeness scale. A supersymmetric modification of this model allows for lighter top masses (M>140), and a scheme with a fourth generation removes the constrains on m(top) entirely.[58]

More Predictions

A recent paper by Osland and Wu[59], uses the absence of certain divergences in the Standard Model to predict

$$M_{top} \approx 120 \text{ GeV} ,$$
$$M_{Higgs} \approx 190 \text{ GeV} .$$

The approach is similar to a relation derived by Veltman[60] which predicted

$$m_e^2 + m_\mu^2 + m_\tau^2 + 3(m_u^2 + m_d^2 + m_c^2 + m_s^2 + m_b^2 + m_t^2) = \frac{3}{2}m_W^2 + \frac{3}{4}m_Z^2 + \frac{3}{4}m_H^2 .$$

The new relations in the Osland Wu approach are

$$m_e^2 + m_\mu^2 + m_\tau^2 + 3(m_u^2 + m_d^2 + m_c^2 + m_s^2 + m_b^2 + m_t^2) = \frac{15}{2}m_Z^2 - 3m_W^2 ,$$

and

$$m_H^2 = 9m_Z^2 - 6m_W^2 .$$

The relations are similar to those which come from demanding loop cancellations in supersymmetry.

All of these are interesting relationships which of course can only be tested after the t quark has been found and its mass measured. They are nevertheless interesting examples of what should be our primary interest in the top quark (assuming it does indeed exist), and that is the possibility of predicting its mass within some theory and gaining an increased understanding of the fundamental mechanisms which are involved in the generation of mass either through the Higgs mechanism or otherwise.

Summary

Let me close these lectures with a few very general remarks in summary. First, we have seen that the evidence in favor of the top's existence is very strong, and that the top is probably quite heavy. There remains some possibility that the top is light and that it has supersymmetric decays which are difficult to detect because of suppression by a heavy LSP. The more standard view is that the top is quite massive. Second, we have learned from Monte Carlo studies that the heavy top has experimental signatures which are sufficiently distinct that we should be able to find it either at the Tevatron if it is light enough, or at the LHC/SSC which are likely to be top factories. Third, the mass of the top is intimately connected to the mass of the Higgs even in the Standard Model, and as we have seen, the connection to the Higgs mechanism may be even more fundamental.

Finally, we can take a quick look at what might be the future of this subject. If the experimental situation were such that I could have told you the mass of the top in these lectures, then we would, I think, first be trying to understand why the top is so heavy while the rest of the quarks are light. Is the top interesting because it is heavy, or are the other quarks interesting because they are so light? Without a theory of quark mass generation, we can't tell. What about the value which we find for the mass of the top; will the mass of the top give us a clue to the location of the Higgs mass? Will the top and Higgs mass be inconsistent with the Standard Model? Will the top mass eliminate some theoretical models? Well, maybe yes, maybe no. But in either case I think you can see that we are not done with the top quark just yet, and this subject which has fascinated us for so long still has an interesting future.

References

[1] G. L. Kane and M. E. Peskin, Nucl. Phys. B195 (1989) 29.

[2] A. Bean et al., Phys. Rev. D35 (1987) 3533;
UA1, C. Albajar et al., Phys. Lett. B262 (1991) 163.

[3] J. Carter, Lepton Photon Conference, Geneva, July 1991.

[4] G. L. Kane and M. E. Peskin, Nucl. Phys. B195 (1982) 29.

[5] M. K. Gaillard and B. W. Lee, Phys. Rev. D10 (1974) 897.

[6] C. Kim, J. Rosner, and C. Yuan, Phys. Rev. D42, 96 (1990).

[7] L. F. Song (CDF), Phys. Rev. Lett. D67 (1991) 3351.

[8] A. A. Akhundov, D. Y. Bardin, and T. Riemann, Nucl. Phys. B276 (1986) 1;
W. Beenakker and W. Hollik, Z. Phys. C40 (1988) 141;
J. Bernabeu, A. Pich, and A. Santamaria, Phys. Lett. B200 (1988) 569.

[9] F. Gilman and Y. Nir, Ann. Rev. Nucl. Part. Phys. 40 (1990) 213;
G. Buchalla, A. Buras, and M. Harlander, Nucl. Phys. B337 (1990) 313.

[10] G-L. Lin, J. Liu, and Y-P. Yao, Mod. Phys. Lett. A6 (1991) 1333.

[11] D. Schaile, CERN-PPE/91-187 (November 1991).

[12] J. Carter, Int. Lepton-Photon Symposium, Geneva, 1991;
J. Ellis, Int. Lepton-Photon Symposium, Geneva, 1991.

[13] P. Langacker, Phys. Rev. Lett. 63 (1989) 1920;
J. Ellis and G. L. Fogli, Phys. Lett. B232 (1989) 139;
J. Ellis and G. L. Fogli, CERN TH/5862 (1990).

[14] CDF Collaboration, 25th Rencontre de Moriond.

[15] R. K. Ellis, Phys. Lett. 259B (1991) 492.

[16] F. Gilman and R. Kauffman, Phys. Rev. D37 (1988) 2676.

[17] T. Rizzo, MAD/PH/637, April, 1990.

[18] H. Plothow-Besch, CERN-PPE/90-168 (1990).

[19] M. Chanowitz, M. Furman, and I. Hinchliffe, Phys. Lett. B78 (1978) 285;
W. Marciano, G. Valencia, and S. Willenbrock, Phys. Rev. D40 (1989) 1725.

[20] J. Ellis, A. Linde, and M. Sher, Phys. Lett. B252 (1990) 203;
H. Zaglauer, Phys. Lett. B206 (1988) 527.

[21] P. Langacker, Univ. of Pennsylvania Report UPR-0435T (1990);
V. Barger, J. Hewett, and T. Rizzo, Phys. Rev. Lett. 65 (1990) 1313;
T. Rizzo, MAD/PH/608(1990).

[22] F. Abe et al., Phys. Rev. Lett. 64 (1990) 142;
F. Abe et al., Phys. Rev. D43 (1991) 664.

[23] F. Abe et al., Phys. Rev. Lett. 64 (1990) 147.

[24] B. Lampe and T. Sack, Phys. Lett. B272 (1991) 339.

[25] E. Reya et al., CERN 90-10 (1990) 304.

[26] G. Altarelli, M. Diemoz, G. Martinelli, and P. Nason, CERN-TH-4978/88, Feb. 1988, Nucl. Phys. B308 (1988) 724.

[27] G. L. Kane, G. A. Landinsky, and C-P. Yuan, SSCL-486 (June 1991).

[28] R. K. Ellis, Phys. Lett. B259 (1991) 492.

[29] M. Diemoz, F. Ferroni, E. Longo, and G. Martinelli, Z. Phys. C39 (1988) 21.

[30] P. Harriman, A. Martin, R. Roberts, and W. Stirling, RAL-90-007 (1990).

[31] F. Cavanna, D. Denegri, and T. Rodrigo (ECFA 1990 LHC Workshop) CERN-PPE/91-25.

[32] R. Hollebeek and P. Sinervo, Snowmass 90.

[33] R. Hollebeek, H. Williams, and P. Sinervo, SDC-90-00117.

[34] R. P. Kauffman, Phys. Rev. D41 (1990) 3343.

[35] DESY 91-153, December 1991.

[36] J. Rossbach, DESY M91-02, 1991.

[37] See W. Kwong, Phys. Rev. D43 (1991) 1488;
M. J. Strassler and M .E. Peskin, Phys. Rev. D43 (1991) 1500.

[38] I. Bigi, Y. Dokshitzer, V. Khoze, J. Kuhn, and P. Zerwas, Phys. Lett. 181B (1986) 157.

[39] Thanks to J. Hewett for pointing out most of this to me.

[40] DESY 91-140.

[41] M. Strassler and M. Peskin, Phys. Rev. D43 (1991) 1500.

[42] A. Djouadi, J. Kalinowski, and P. Zerwas, DESY 91-104.

[43] D. P. Roy CERN-TH.6247/91;
R. M. Godbole and D. P. Roy, Phys. Rev. D43 (1991) 3640.

[44] UA1 Collaboration: M. Felini, Proc. of the 8th Topical Workshop, Castiglione, Sept. 1989.

[45] C. Albajar et al., Phys. Lett. B257 (1991) 459.

[46] UA2 Collab., Phys. Lett. B280 (1992) 137.

[47] Z. Kunzt, Z. Trocsanyi, and W. Stirling, ETH-TH/91-17;
A. Ballestrero and E. Maina, Phys. Lett. B268 (1991) 437.

[48] F. Gilman and R. Kauffman, Phys. Rev. D37 (1988) 2676.

[49] P. Zerwas, DESY 91/108, p. 24.

[50] For further discussion, see:
A. Czarnecki, M. Jezabek, and J. Kuhn, Nucl. Phys. B351 (1991) 70;
G. Kane, G. Ladinsky, and C-P. Yuan, Phys. Rev. D45 (1992) 124;
R. Dalitz and G. Goldstein, Phys. Rev. D45 (1992) 1531.

[51] A. Blinov, V. Khoze, and N. Uraltsev, DESY 88-102.

[52] C. Peterson, D. Schlatter, I. Schmitt, and P. Zerwas, Phys. Rev. D27 (1983) 105.

[53] Y. Dokshitzer, V. Khoze, and S. Troyan, LU-TP-92-10, Mar. 1992.

[54] T. Sjostrand and P. Zerwas, CERN-TH.6313/91.

[55] N. Krasnikiv and S. Pokorski, CPTH-A164-0492 (1992) Apr.

[56] H. Baer, M. Drees, R. Godbole, J. Gunion, and X. Tata, Phys. Rev. D44 (1991) 725.

[57] Christopher Hill Fermi-Pub-92/19-T, Jan. 15, 1992;
W. A. Bardeen, C. T. Hill, and M. Lindner, Phys. Rev. D41 (1990) 1647.

[58] See also:
A. Hasenfratz, P. Hasenfratz, K. Jansen, J. Kuti, and Y. Shen, Nucl. Phys. B365 (1991) 79;
V. Miransky, M. Tanabashi, and K. Yamawaki, Phys. Lett. B221 (1989) 177;
V. Miransky, M. Tanabashi, and K. Yamawaki, Mod. Phys. Lett. A4 (1989) 1043;
K. Yamawaki, DPNU-92-04, Jan. 1992.

[59] P. Osland and T. T. Wu, Bergen 1992-02 Harvard-DAS-92/1.

[60] M. Veltman, Acta Physica Polonica B12 (1981) 437.